



# **POLITECNICO DI TORINO**

*Department of Environment, Land And Infrastructure Engineering*

Master of Science in Petroleum and Mining Engineering

## **Master's Degree Thesis**

### **Modeling and analysis of co-axial borehole heat exchanger for the heat production from the depleted/exploratory hydrocarbon wells**

Candidate: Najeeb Ahmad

Supervisors: Prof. Stefano Lo Russo (Politecnico di Torino)  
Prof. Mohsen Assadi (University of Stavanger)  
Prof. Martina Gizzi (Politecnico di torino)

**Academic year: 2020-2021**

# ACKNOWLEDGEMENT

I'd like to convey my heartfelt appreciation to Prof. Stefano Lo Russo, the thesis's supervisor, for allowing me to complete this research and for his recommendations and availability. I would like to thank Prof. Martina Gizzi and Prof. Mohsen Assadi (University of Stavanger) for their assistance and useful ideas during the thesis process.

A particular thanks to my parents, who sacrificed so much to allow me to achieve this dream. Throughout the entire course of my education, they have always supported me and, more importantly, persevered with me, allowing me to grow and become the person I am today.

Thank you to my best pals Irfan Khan and Animesh Chalga for always being by my side. They pushed me to always do my best with their unwavering support, but most importantly by their compassion and faith in me. Thank you to all of my Politecnico colleagues who supported me over these years.

# Abstract

The heat beneath our feet, as a geothermal energy resource, seems to have the potential to provide a portion of the world's energy demands, whether by direct heat offer or power generation. The major research challenge has been to develop a technique to economically and efficiently collect thermal energy from the ground. Drilling new geothermal wells, which cost over half of the plant's total budget, is a major limitation in allocating money. There are millions of abandoned/exploratory hydrocarbon wells, however, that can be used to collect heat from the ground. These existing hydrocarbon wells can be regarded as a viable option since most of them have the capacity to generate enough heat for direct consumption and power generation. However, we must determine which wells can produce enough heat energy in a safe, flexible, and cost-effective manner.

Both the scientific community and industry have shown an increased interest in geothermal energy in recent years. In this thesis work, we chose two exploratory hydrocarbon wells located in northern Italy as case studies: CASTEGGIO Well in the province of Pavia, Lombardia, and TURBIGO Well in the province of Milan, Lombardia. In order to draw heat from the bottom of the well, a simplified co-axial wellbore heat exchange model is used, with water flowing downward via the exterior pipe and returning through the inner tube. The influence of several typical characteristics of the rocks, such as thermal conductivity, specific heat capacity, and density, on the quantity of heat extracted, was investigated using an existing simplified analytical model by using MATLAB software. A sensitivity study was also performed by changing the fluid's inlet flow rate and temperature, outer pipe diameter, insulating material and thickness of the inner pipe. As the wells' locations are already known, this study could make use of accessible geological data, a temperature profile, and a geothermal gradient.

The goal of this study is to determine if the identified hydrocarbon wells have enough potential to be turned into geothermal wells, either for power generation or direct consumption, using co-axial borehole heat exchangers technology. Additionally, in order to tap the geothermal energy at the surface to its complete potential, an analysis is done on the parameters influencing the heat extraction rate for different scenarios in both wells of varied geological formations, depths, and geothermal gradients.

The inferences drawn based upon results have shown that the thermal energy extracted from the wells depends primarily on the circulating inlet fluid flowrate and temperature, depth of the well (temperature of rocks varies and increases with depth), geothermal gradient, thermal conductivity and thickness of insulation of the central pipe. The research also outlines that in comparison to the other factors, the impact of outer diameter is important but slightly less significant in our study; and the influence of heat conductivity of rocks rises with the increase in depth of the well that has a greater impact on TURBIGO Well. Basis comparison of the above parameters, and the direct effect of differences in depth and geothermal gradient on the outlined parameters, we observed that TURBIGO is more effective in terms of electricity generation as opposed to CASTEGGIO. For an in-depth assessment to determine the viability

of electricity generation and direct use of thermal energy would require further cost analysis for both the considered wells.

# Index

1.1	Introduction to the research work .....	8
1.2	Introduction to geothermal energy .....	9
1.3	Geothermal energy resources in oilfields .....	10
1.4	Italian Petroleum Systems .....	11
1.5	Methods of extracting geothermal resources from oilfields .....	14
1.6	Vertical Ground Heat Exchangers (GHEs) .....	16
1.7	Applications of Geothermal Resource .....	17
1.8	Geothermal Power plants .....	20
2.	MATERIALS AND METHODS .....	23
2.1	Coaxial borehole heat exchanger .....	23
2.2	Wells Description .....	24
2.3	Analytical models .....	28
2.4	Heat transfer model used in our thesis work .....	32
3.	RESULTS & DISCUSSIONS .....	37
4.	COMPARISON BETWEEN THE WELLS .....	61
5.	CONCLUSIONS .....	63
	<b>REFERENCES</b> .....	<b>65</b>

# List of Figures

Figure 1: geographic location of five petroleum systems recognised in Italy (above right), stratigraphic distribution of related source rocks and hydrocarbon occurrences (above left), and relationships b/w hydrocarbon occurrences & techno-stratigraphic settings [14].....	13
Figure 2: Oil & Gas wells in Italy. (A) The complete collection, (B) Only active wells in Italy in 2019 [18] .....	14
Figure 3: Schematics of produced fluid flow for geothermal extraction from production wells [9] .....	15
Figure 4: Common vertical GHE designs [20] .....	16
Figure 5: Schematic of different types of ground source heat pumps [20] .....	18
Figure 6: Residential Heat Pumps .....	18
Figure 7: Modified Lindal Diagram (Based on [22,23]) .....	19
Figure 8: Single Flash Power Plant [25].....	20
Figure 9: Dual Flash Power Plant [25].....	21
Figure 10: Binary Flash Power Plant [25].....	22
Figure 11: Co-axial Borehole heat Exchanger [28].....	24
Figure 12: Litho-stratigraphic profile of CASTEGGIO (data derived from the Italian National Geothermal Database).....	25
Figure 13: Temperature Profile of CASTEGGIO (DATA DERIVED FROM THE ITALIAN NATIONAL GEOTHERMAL DATABASE).....	26
Figure 14: Litho-stratigraphic profile of TURBIGO (DATA DERIVED FROM THE ITALIAN NATIONAL GEOTHERMAL DATABASE).....	27
Figure 15: temperature profile of TURBIGO (DATA DERIVED FROM THE ITALIAN NATIONAL GEOTHERMAL DATABASE).....	28
Figure 16: Schematic of Line Source Model .....	29
Figure 17: Schematic of Cylindrical Source Model .....	30
Figure 18: Schematic representation of heat transfer in co-axial heat exchangers [35].....	33
Figure 19: Case A- Inlet flowrate = 3 kg/s, outlet temp = 39.5°C, inlet temp = 30°C.....	37
Figure 20: Case B- Inlet Flowrate = 0.5 kg/s, Outlet temp = 55.8°C, Inlet temp = 30°C.....	38
Figure 21: Variation in Outlet temp as inlet flowrate changes.....	39
Figure 22: Heat Power vs Inlet Fluid Rate.....	39
Figure 23: Case A- $T_{INLET} = 30^{\circ}C$ , $T_{OUTLET} = 39.5^{\circ}C$ , Flowrate = 3 kg/s .....	40
Figure 24: Case B- $T_{INLET} = 40^{\circ}C$ , $T_{OUTLET} = 44.8^{\circ}$ , Flowrate = 3 kg/s .....	40
Figure 25: Case C- $T_{INLET} = 40^{\circ}C$ , $T_{OUTLET} = 44.8^{\circ}$ , Flowrate = 3 kg/s .....	41
Figure 26: Variation in outlet temp with change in inlet temp .....	41
Figure 27: Heat power variation as inlet temperature changes.....	42
Figure 28: Case A- Outlet temperature = 39.5°C .....	43
Figure 29: Case B- Figure 25 (B): Outlet temperature = 42°C.....	43
Figure 30: Case A- Outlet Temp = 39.5°C, Q = 120.14 kW .....	44
Figure 31: Case B- outlet temp = 40°C, Q = 126.46 kW .....	45
Figure 32: Case A- $T_{out} = 32.2^{\circ}C$ @ $\lambda = 0.25^{\circ}C$ , $T_{inlet} = 30^{\circ}C$ , flowrate = 0.5 kg/s.....	46
Figure 33: Case B- $T_{out} = 55.8^{\circ}C$ @ $\lambda = 0.025$ W/m.K, flowrate = 0.5 kg/s, $T_{inl} = 30^{\circ}C$ .....	46
Figure 34: Case A - $T_{out} = 36.4^{\circ}C$ @ flowrate = 3 kg/s & Thermal conductivity = 0.25 W/m.K.....	47
Figure 35: Case B - $T_{out} = 39.5^{\circ}C$ @ flowrate = 3 kg/s & Thermal conductivity = 0.025 W/m.K.....	47
Figure 36: Case A - $T_{inlet} = 30^{\circ}C$ , Flowrate = 0.5 kg/s, $T_{outlet} = 120^{\circ}C$ .....	49
Figure 37: Case B - $T_{INLET} = 30^{\circ}C$ , Flowrate = 1 kg/s, $T_{OUTLET} = 126^{\circ}C$ .....	49
Figure 38: Case C - $T_{inlet} = 30^{\circ}C$ , Flowrate = 1.5 kg/s, $T_{outlet} = 120^{\circ}C$ .....	50
Figure 39: Case D - $T_{inlet} = 30^{\circ}C$ , Flowrate = 3 kg/s, $T_{outlet} = 98^{\circ}C$ .....	50
Figure 40: Variation in outlet temp as flowrate changes .....	51
Figure 41: Heat Power vs Flowrate.....	51
Figure 42: case A - $T_{inlet} = 30^{\circ}C$ , Flowrate = 3 kg/s. $T_{outlet} = 98^{\circ}C$ .....	52
Figure 43: Case B - $T_{inlet} = 80^{\circ}C$ , Flowrate = 3 kg/s. $T_{outlet} = 110.9^{\circ}C$ .....	53
Figure 44: Variation in outlet temp as inlet temperature changes .....	53

Figure 45: Heat Power changes almost linearly with inlet temperature.....	54
Figure 46: Case A - Tinlet = 30°C, Flowrate = 3 kg/s, Toutlet = 98°C .....	55
Figure 47: Case B - Tinlet = 30°C, Flowrate = 3 kg/s, Toutlet = 113.6°C.....	56
Figure 48: Case A - Tinlet = 30°C, Flowrate = 3 kg/s, Toutlet = 98°C .....	57
Figure 49: Case B - Tinlet = 30°C, Flowrate = 3 kg/s, Toutlet = 100°C.....	57
Figure 50: Case A - Thermal conductivity = 0.025 W/m.K, Toutlet = 98°C .....	58
Figure 51: Case B - Thermal conductivity = 0.25 W/m.K, Toutlet = 61°C.....	58
Figure 52: Outlet temperature variation with Thermal conductivity of insulated Centre pipe .....	59
Figure 53: Heat Power trend vs thermal conductivity of inner pipe .....	59

# INTRODUCTION

## **1.1 Introduction to the research work**

The energy contained beneath the surface of the earth can play a critical role in meeting the world's energy needs since it has the potential to provide enough energy for the entire planet because it is one of the most abundant renewable energy sources and is widely regarded as a constant and independent source of energy.

There are millions of abandoned/exploratory wells that are already drilled, can be used to extract heat by installing the wellbore heat exchangers. Because drilling expenditures may account for more than half of a geothermal project's overall cost, utilising depleted and abandoned gas and oil wells is a smart way to cut those costs. These systems can be utilised for direct room heating and cooling, combined with heat pumps, industrial use or even in power generation systems, depending on the temperature reached in the Deep Borehole Heat Exchanger. There are innovative non-traditional heat extraction technologies, such as the Enhanced Geothermal System (EGS), Combined Heat and Power System (CHPs), and Advanced Geothermal System (AGS) that employ closed-loop Borehole Heat Exchangers (BHEs).

Borehole heat exchangers can be installed in a variety of designs such as single U-tube, double U-tube, Co-axial (tube-in-tube assembly) or Wellbore heat exchanger (WBHX), energy piles, and so on. Our research mainly focuses on co-axial borehole heat exchangers. It is a tube-in-tube assembly consisting of outer and inner pipes in which the working fluid is injected into the annulus and withdrawn via the insulated inner tubing, resulting in a reverse circulation. The working fluid inside the annulus extracts heat from the heated wellbore to the surface via heat convection and heat conduction to create thermal energy that may then be utilised to generate geothermal electricity, space and district heating, spa and swimming pool heating, greenhouse and soil heating, aquaculture pond heating, industrial process heating and snow melting, etc.

In this research, we selected two offshore exploratory hydrocarbon wells in the northern part of Italy as case studies and applied an existing approach in MATLAB software for the co-axial borehole heat exchangers to determine the effects of various rocks and wellbore characteristics on the heat extraction process. The most important point is how to extract heat economically and efficiently from wells, which is based on various technical parameters of the wellbore such as fluid inlet temperature, injecting fluid flow rate, thickness and thermal conductivity of thermal inner tube insulation, depth of the well, geothermal gradient, and the physio-chemical properties of rocks such as thermal conductivity, specific heat capacity, and density. These rocks characteristics vary depending on the geological context of the earth. After the investigation of all the parameters concerned with the wellbore and underground formations, a conclusion is made whether these two chosen wells have enough potential to convert them into geothermal one.



## **1.2 Introduction to geothermal energy**

Geothermal energy is the thermal energy stored in the form of heat beneath the earth's surface. It is a constant and independent form of renewable energy and plays a key role towards the world's future energy balance. In particular, deep geothermal resources are largely available across continents and can help countries become less dependent on energy imports and build a broader base in their future energy mix. However, despite its significant potential, the total contribution of the geothermal sector to global power generation remains relatively small. According to the International Energy Agency's (IEA) roadmap [1], geothermal power generation may reach 1 400 TWh per year by 2050, accounting for around 3.5 percent of worldwide electricity production. By 2050, geothermal heat may generate 5.8 EJ per year.

Although the use of geothermic hot springs has been documented since ancient times, significant geothermal investigation for industrial reasons began in the early nineteenth century in Larderello with the use of geothermal fluids (boric acid) (Italy). The first geothermal district heating system was installed in the United States towards the end of the nineteenth century, with Iceland following suit in the 1920s. The first successful system to create power from geothermal heat was established in Larderello around the turn of the twentieth century. Installed geothermal power has continuously risen since then. Until recently, the use of earth's heat was limited to areas where geological characteristics permitted a high-temperature circulating fluid of 100°C to 300°C to extract heat at a depth [1].

Meanwhile, there are 20-30 million abandoned oil wells around the world [2]. These abandoned oil wells have a large amount of heat energy and can be changed into geothermal wells by a double-pipe heat exchanger for power generation [3-6]. Existing wells also offer the opportunity to extend the length of drilled wells to a deeper depth or drill a lateral to access improved thermal conditions or geothermal reservoirs farther away. In addition, providing further use of abandoned wells can eliminate liabilities related to plug and abandonment, because abandoning a well is a high-cost process. In consequence, most wells are done at a minimal cost and they meet the minimal obligations set by regulating agencies. In this way, the cost of drilling can be reduced and pollution problems of abandoned oil can be solved. It is a new way to utilize geothermal energy.

Geothermal energy has the potential to supply more energy than the global total of oil and natural gas combined. It is renewable, stable, and has a minimal carbon footprint. Geothermal power plants can produce electricity consistently, constantly, and without regard to weather conditions. The power output of a geothermal power plant can be accurately predicted, and the actual power output is very close to total installed capacity. Yet, current global geothermal energy use comprises only 1% of energy production [7].

Geothermal energy may be collected from either deep geothermal resources, which generally extend kilometers beneath the ground level, or shallow geothermal resources, which reach just a few hundred meters beneath the earth's surface. Deep geothermal resources are formed by heat transported from the Earth's core as well as nuclear reactions in deep geological formations. These geothermal resources may be utilised to generate geothermal electricity, heat buildings and districts, heat spas and swimming pools, heat greenhouses and

soil, heat aquaculture ponds, heat industrial processes, and melt snow. Shallow geothermal energy, which is mostly derived from passively stored solar energy, may be utilised for both heating and cooling. Heat or cold is actively stored in the ground in certain systems, which use a range of sources such as solar radiation, interior air, outdoor air, or thermal waste from industrial activities. Heat pumps are used in the vast majority of shallow geothermal systems. Shallow geothermal energy systems can store thermal energy throughout a season [8].

Geothermal energy may offer low-carbon base-load electricity and heat from high-temperature hydrothermal resources, low- and medium-temperature deep aquifer systems, and hot rock resources. It is considered renewable because there is a continual terrestrial heat movement from the vast heat stored beneath the Earth to the surface, then to the atmosphere. Heat may be removed at various rates. The utilisation of geothermal energy on a long-term basis requires that the heat extracted from the resource is replenished on a comparable period. Practical replenishment (e.g., 95 percent recovery) will typically be achieved on time scales of the same order as the geothermal producing system's lifetime. It is proposed that there exists a specific threshold of maximum energy output for each geothermal system and method of production, below which it will be feasible to sustain steady energy production from the system for 100 to 300 years.

### **1.3 Geothermal energy resources in oilfields**

Geothermal energy is a renewable and sustainable energy source that is weather independent, steady, and ecologically beneficial. The utilisation of geothermal energy can help to minimise global warming, reduce air pollution, and fulfil world energy consumption needs. For decades, geothermal energy was mostly used in areas with a high geothermal gradient and intense volcanic activity or hydrothermal resources, such as geysers in the United States and Iceland in Europe. Furthermore, geothermal energy is not limited to such locations, but it also has significant potential in hydrocarbon reserves due to various cost, risk, flexibility, and other advantages.

Geothermal energy may be divided into three categories: low, medium, and high-temperature resources. This categorization represents the availability of various resources that may be used at specific temperatures, such as space heating/cooling, industrial drying, power production, and other uses. Among a variety of categorization approaches, we will utilise the following categories in this case [9-10].

- a) High-temperature resource: above 150°C
- b) Intermediate temperature resource: between 90°C to 150°C
- c) Low-temperature resource: between 30°C to 90°C

As a type of resources that co-exist with hydrocarbon in sedimentary basins, oilfield geothermal resource falls into the intermediate to low temperature category given that the produced fluids temperatures range between 65°C and 150°C [11].

When compared to typical geothermal fields, oilfields may provide significant benefits for developing geothermal energy using existing wellbores and facilities at a minimal cost and risk. Production of geothermal energy from oilfields is an excellent alternative for reducing

capital expenditure in drilling and well integrity. There is already enough geological data for abandoned and exploratory hydrocarbon wells that have been gathered during production or exploration. The existing wellbore would reduce the significant expense and risk associated with drilling and completion activities.

Oilfields contain a significant number of candidate wells for geothermal energy generation since most hydrocarbon reservoirs are diminishing and have been abandoned owing to inadequate oil production and the production of a large volume of water. Exploratory hydrocarbon wells have the potential to generate a significant quantity of geothermal energy. Among a sufficient number of candidate wells, operators might select the well with the highest bottom hole temperature to supply the quantity of heat that can be advantageous for future purposes such as direct usage, power production, or industrial uses.

It is widely known that oil firms are not only huge energy producers, but also large energy consumers; they use a large quantity of gas, oil, and coal to heat living spaces, conduct thermal recovery of heavy oil, and give warmth to oil pipelines, among other things. This use of gas and oil raises not just operational expenses but also living costs. Exploiting and using existing oilfield thermal resources has the potential to not only replace oil, gas, coal, and other fossil fuels, but also to give a new path for oilfield economic diversification and future growth. As a result, the extraction and usage of oilfield geothermal energy have a promising future. [12]

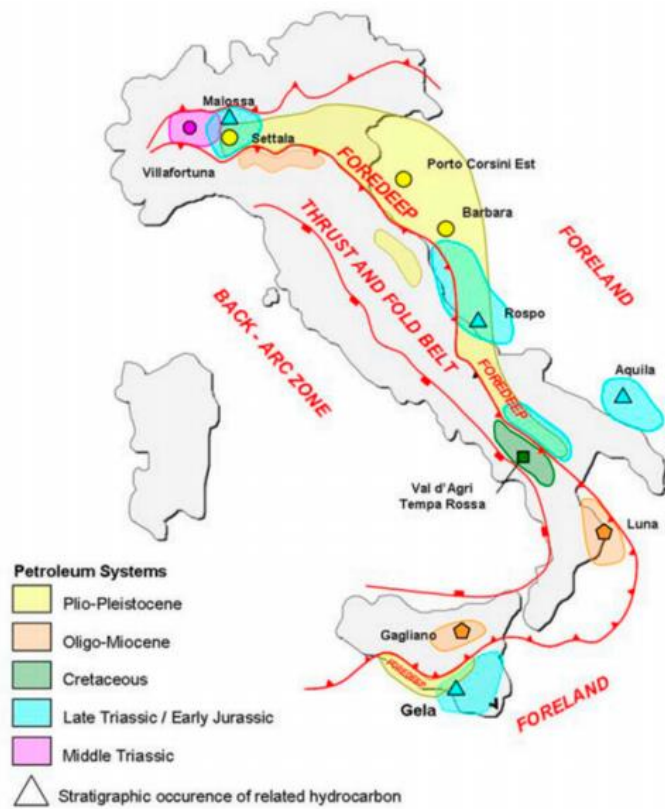
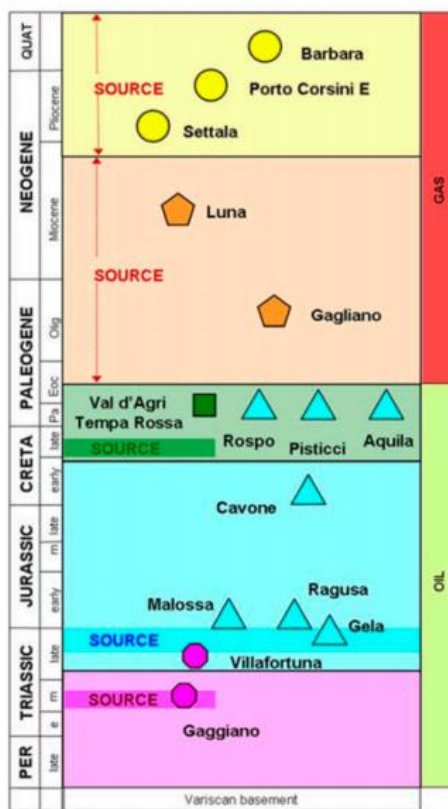
#### **1.4 Italian Petroleum Systems**

Carbonate and siliciclastic reservoir rocks ranging in age from the Triassic to the Paleogene and from the Oligocene to the Pleistocene, respectively, are associated with hydrocarbon occurrences in Italy (fields, discoveries, and shows), which are distributed in thrust belt, foredeep basin, and foreland geological settings. (Figure 1).

At least five major petroleum systems [13] may be identified in Italy based on the primary source rocks [14,15-17] and references therein). Figure 1 depicts the approximate geographic range of these petroleum systems, as well as the stratigraphic distribution of known source rocks and hydrocarbon discoveries. Three of these petroleum systems, all of which are oil-prone, are linked to Mesozoic passive margin sedimentary covers composed of shallow sea and pelagic carbonates, evaporites, and clastic sediments deposited after the Mesozoic extensional tectonic phases. The final two petroleum systems, which are mostly gas-prone, are instead associated with terrigenous Oligo-Miocene and Plio-Pleistocene foredeep strata deposited during the formation of the Alpine and Apennine orogens. Table 1 summarises the key characteristics of these five petroleum systems.

Table 1. Italian petroleum system and typical associated fields.

Petroleum System	Reservoir Source Rock	Representative Fields
Middle Triassic	Fractured and dolomitized shelf carbonates, hosted in trust-related folds and sealed by marly and volcanoclastic units, are charged by the Besano Shales (Anisian/Ladinian) and Meride Limestone (Ladinian) source rocks.	Villafortuna-Tredate oil field, discovered in 1984 with a cumulative production at the end of 2000 of 188 Mbo of 43° API oil and more than 2000 MSTm3 of gas.
Late Triassic–Early Jurassic	Oil accumulations in a variety of stratigraphic intervals of the Mesozoic–Early Cenozoic sedimentary cover overlying Late Triassic–Early Jurassic source rocks in traps generally represented by reactivated structures occurring along the foreland margin.	Gela oil field in Sicily discovered in 1956 with reserves of 130–150 Mbo.
Cretaceous	The reservoir is made up by Cretaceous–Middle Miocene fractured shallow-water limestone and dolostones sealed by shaly units in traps represented by thrust-related folds. It is charged by an Albian–Cenomanian organic-rich carbonate source rock deposited in isolated basins developed during the Cretaceous anoxic events within the long-lasting Apulian carbonate platform.	Val d’Agri oil field, discovered in 1988 with estimated reserves of about 480 Mbo of 26°–42° API oil.
Thermogenic gas in Oligo-Miocene foredeep	This system is associated with an early thermogenic generation from the gas-prone organic matter contained in the shaly levels that charged the turbidite reservoirs. Hydrocarbon accumulations hosted in structural traps with some light oil and condensate.	Typical examples are the Gagliano and Luna gas fields.
Biogenic gas in Plio-Pleistocene foredeep	The sand-rich turbidite reservoir is charged with biogenic gas by the interbedded clay levels, characterised by an organic matter of terrestrial origin, which also provides the seal. Traps are usually structural although several stratigraphic traps have been also recognised.	Porto Corsini East and Barbara gas fields.



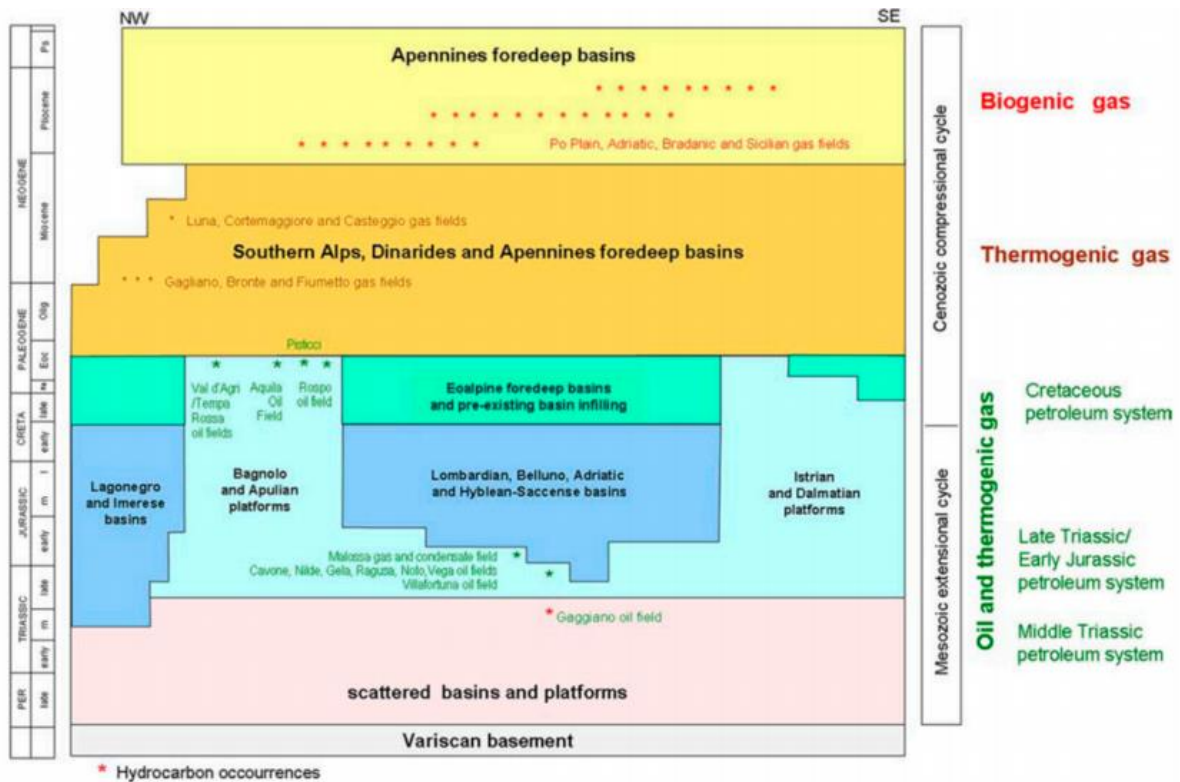


FIGURE 1: GEOGRAPHIC LOCATION OF FIVE PETROLEUM SYSTEMS RECOGNISED IN ITALY (ABOVE RIGHT), STRATIGRAPHIC DISTRIBUTION OF RELATED SOURCE ROCKS AND HYDROCARBON OCCURRENCES (ABOVE LEFT), AND RELATIONSHIPS B/W HYDROCARBON OCCURRENCES & TECHNO-STRATIGRAPHIC SETTINGS [14]

The MISE reported, at the end of November 2019, 93 research permits and 193 production concessions, while the active hydrocarbon wells (as of February 2019) numbered 2166 in total, of which 898 were located onshore with a productive or potentially productive operational status (Figure 2) [18].

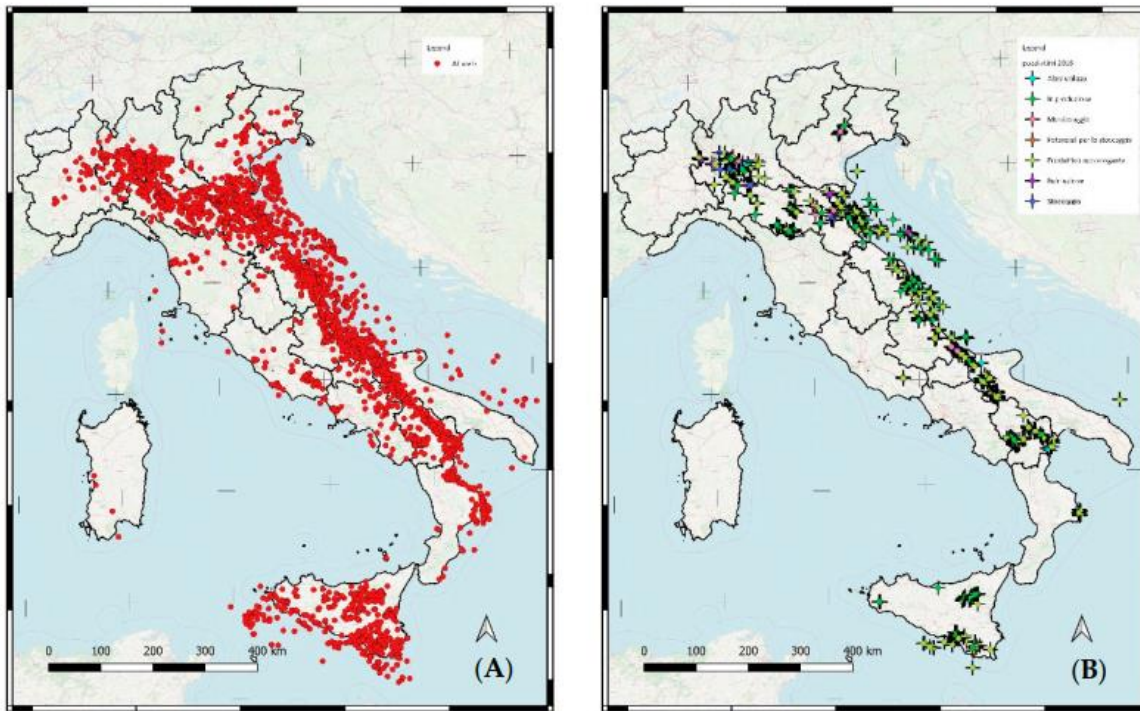


FIGURE 2: OIL & GAS WELLS IN ITALY. (A) THE COMPLETE COLLECTION, (B) ONLY ACTIVE WELLS IN ITALY IN 2019 [18]

### **1.5 Methods of extracting geothermal resources from oilfields**

There are a variety of methods for obtaining geothermal heat from the subsurface, including water co-production during oil and gas extraction, borehole heat exchangers, enhanced or engineered geothermal systems, ground source heat pumps, and so on. The following are some of the technologies for extracting heat from the ground, in short.

#### **Geothermal extraction by produced water from producing wells**

This process uses geothermally heated formation water, a by-product of oil and gas production. As shown in Figure 3, high-temperature water is produced at the surface alongside hydrocarbons, after which the water is separated and sent to processing facilities to capture the heat, which is then distributed or converted to electricity by a power plant, completing the coproduction of hydrocarbon and geothermal energy. High water production wells are the most common producing wells utilised for geothermal extraction and use. Historically, produced water has been an inconvenience and required costly disposal: however, it is now being looked at as a resource that can be used to produce electricity for field operations or sold to the grid [9].

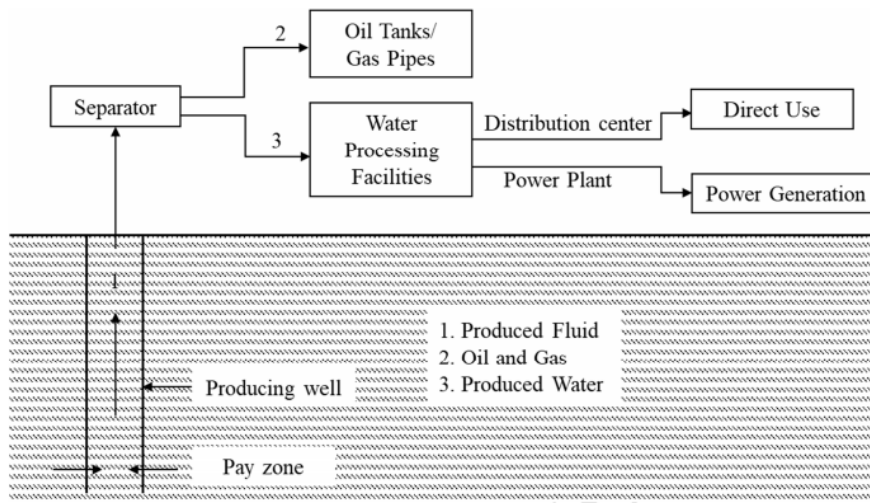


FIGURE 3: SCHEMATICS OF PRODUCED FLUID FLOW FOR GEOTHERMAL EXTRACTION FROM PRODUCTION WELLS [9]

### Geothermal Extraction by working fluid from abandoned wells

Another option is to recover geothermal resources from decommissioned oil wells. Wells will always be abandoned after hydrocarbon reserves have been depleted to the point that they are no longer economically viable. These wells are typically viewed as long-term liabilities, resulting in high plug-and-abandon expenses.

However, because an existing wellbore provides access to a subsurface geothermal resource, an abandoned well might be used to harvest geothermal heat. The idea behind this approach is to pick a depleted petroleum reservoir and repurpose it as a geothermal reservoir, then collect the heat using a working fluid pumped from the surface. Working fluid must be injected to the required depth, acting as a heat extractor and heat transporter, because there are no geofluids provided by the pay zones in abandoned wells. Typically, fluid is injected near the surface, and as it travels down, the fluid is gradually heated by the surrounding formation. The injected fluid changes direction, travels upward, and ascends to the wellhead when it reaches the bottom of the heat exchanger, when it achieves its maximum temperature. At the wellhead, return fluid will be collected, and heat will be recovered and used for various reasons. Before injecting fluids, some wellbore modification may be required to recover heat from abandoned wells. Retrofitting abandoned wells using U-tube and double-pipe heat exchangers is a frequent practice [9].

### Enhanced Geothermal Systems

Geothermal systems that have been enhanced or developed are designed to use the heat of the Earth when there is no or inadequate steam or hot water and where permeability is poor. The focus of EGS technology is on designing and constructing massive heat exchange zones in hot rock. Enhancing permeability includes opening pre-existing fractures and/or generating new fractures. Heat is extracted by pumping a transfer medium, usually water, down a borehole into hot fractured rock and then pumping the heated fluid up another borehole to a power plant, where it is pushed back down (recirculated) to repeat the cycle.

EGS can encompass everything from stimulating existing sites with low permeability to building new geothermal power plants in areas where geothermal fluids do not exist. EGS, also known as hot dry rock technology, has been under development since the initial studies on very low permeability rocks in the 1970s. On the surface, the heat transfer medium (typically hot water) is utilised to create electricity and/or heat in a binary or flash plant [1].

### 1.6 Vertical Ground Heat Exchangers (GHEs)

Borehole Heat Exchangers are another name for Vertical Ground Heat Exchangers. Borehole heat exchangers (BHE) are classified into two types: U-tube and concentric- (coaxial-) tube system designs (Figure 4). When there is a requirement to install adequate heat exchanger capacity under a restricted surface area, such as when the ground is rocky near to the surface, or when little damage to the landscape is required, BHEs are commonly utilised [19]. The U-tube vertical GHE might consist of one, tens, or even hundreds of boreholes, each with a single or double U-tube through which heat exchange fluid is pumped. Concentric pipes are frequently employed in Europe, either in a very simple way with two straight pipes of different diameters or in complex arrangements. The borehole annulus is often backfilled with a specific substance (grout) that prevents ground-water pollution.

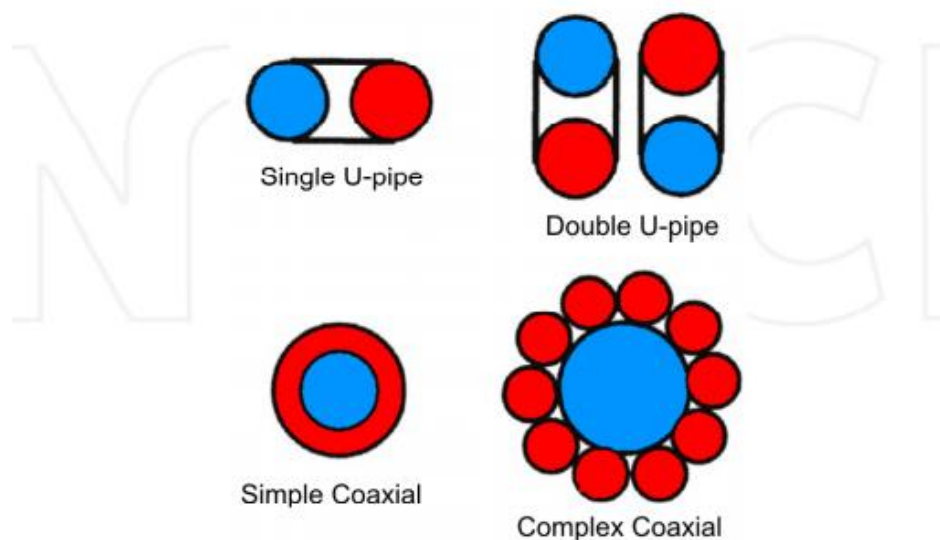


FIGURE 4: COMMON VERTICAL GHE DESIGNS [20]

The borehole heat exchanger (BHE) is a device that extracts heat from shallow and/or deep rock formations without the creation of geofluid. Technically, it is a heat exchanger that is placed within the chosen borehole and circulates any heat-carrying fluid (mostly water) through it. Because BHEs are closed-loop systems, circulating fluids have no interaction with the surrounding formations. This configuration removes the corrosion and scale problems that are commonly associated with enhanced geothermal systems. As a consequence, during geothermal energy generation using BHEs, no water processing equipment is required. Furthermore, BHEs can limit the leakage of carbon dioxide and other fugitive gases. BHEs use



less pumping power and may use a broader range of working fluids than enhanced geothermal systems. Finally, BHEs reduce the possibility of induced seismicity in improved geothermal systems caused by hydraulic fracturing (EGS).

### **1.7 Applications of Geothermal Resource**

Geothermal energy uses can be divided into three categories: direct-use applications, geothermal heat pumps (GHPs), and electric power generation.

#### **Direct Uses**

The most common approach is the direct use of hot water from the ground without the use of any specific apparatus. All direct use applications rely on low-temperature geothermal assets with temperatures ranging between 50 and 150 °C (122 and 302 °F). Low-temperature geothermal water and steam have been used to heat individual buildings as well as whole regions where many structures are heated from a single supply source. Furthermore, geothermal assets have been used to heat numerous swimming pools, balneological (therapeutic) offices at spas, nurseries, and aquaculture lakes across the world. Other direct geothermal energy applications include cooking, mechanical applications (such as drying natural goods, vegetables, and timber), milk sanitization, and large-scale snow melting. Boiling water is commonly used directly in the heating framework for a substantial number of those activities, or it may be used in conjunction with a heat exchanger, which transports heat when hazardous minerals and gases, for example, hydrogen sulphide, are blended in with the liquid. [9]

#### **Geothermal Heat Pumps (GHPs)**

Geothermal heat pumps (GHPs) use the relatively consistent mild temperature conditions that exist within the first 300 meters (1,000 feet) of the surface to heat and cool buildings in the winter and summer.

Below the frost line, the ground temperature is usually stable. In the middle of winter, the ground is warmer than the outside air, and in the middle of summer, it is colder. As a result, the earth is an effective heat source. The temperature of the ground maintains a close constant temperature of 10 to 16 °C (50 to 60 °F) in shallower profundities, where most GHPs are located, for example, inside 6 meters (about 20 feet) of the Earth's surface. As a result, that heat may be used to help warm buildings during the colder months of the year when the air temperature falls below that of the ground. During the hottest months of the year, heated air can also be taken from a structure and routed underground, where it loses a lot of heat and is returned [20].

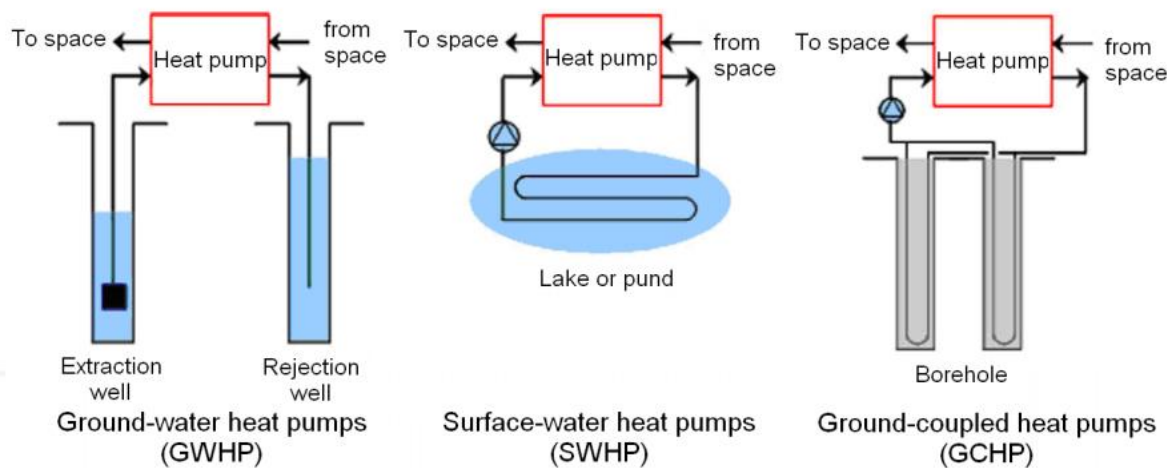


FIGURE 5: SCHEMATIC OF DIFFERENT TYPES OF GROUND SOURCE HEAT PUMPS [20]

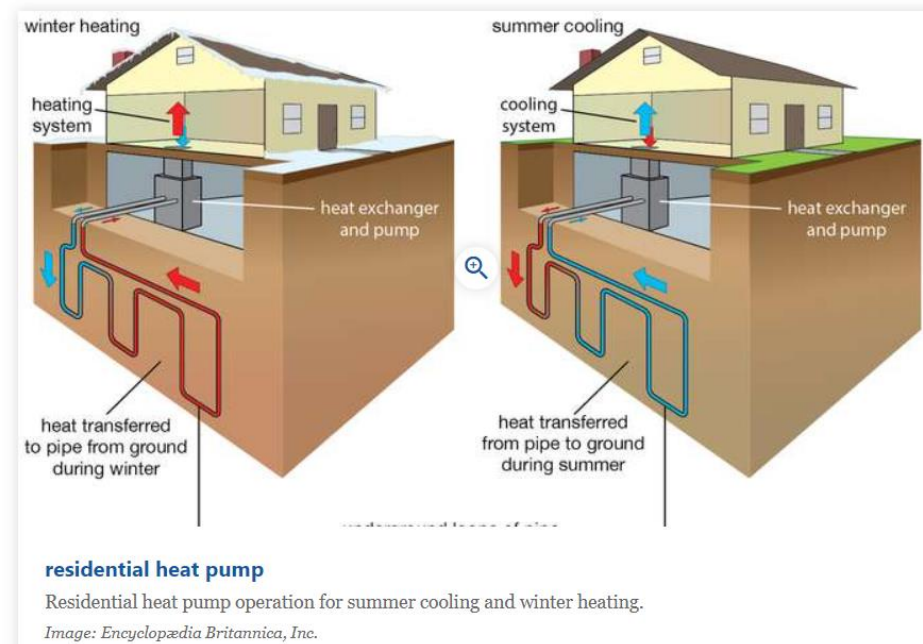


FIGURE 6: RESIDENTIAL HEAT PUMPS

A heat exchanger (a loop of pipes buried in the ground) and a pump comprise a GHP system (Figure 5 & 6). The heat exchanger transmits heat energy between the ground and the air at the surface via a fluid that flows through the pipes; the fluid is frequently water or a mixture of water and antifreeze. The heat from warm air is transported to the heat exchanger and into the fluid during the warmer months. The heat is distributed to the rocks, soil, and groundwater as it passes through the pipes. During the colder months, the pump is reversed. Heat energy accumulated in the comparatively warm earth boosts the fluid's temperature. The fluid then transfers this energy to the heat pump, which warms the air inside the building.

## Electric Power Generation

Geothermal energy may be utilised to create power depending on the temperature and fluid (steam) flow. Electricity may be generated by geothermal power plants in three ways. Despite its structural differences, all three regulate the behaviour of steam and utilise it to power electrical generators. Geothermal power is considered a kind of renewable energy since the extra water vapour after each operation is condensed and returned to the earth, where it is warmed for later use.

Some geothermal power facilities merely collect rising ground steam. The heated water vapour is funnelled straight into a turbine, which operates an electrical generator in such "dry steam" operations. Other power plants, based on the flash steam and binary cycle designs, begin the electrical production process with a mixture of steam and warm water ("wet steam") collected from the ground.

The variety of possible applications, together with the corresponding temperature demand, is illustrated by the Lindal diagram shown in Figure 7. By cascading exploitation of the heat accumulated in utilising geothermal water we mean a multi-variant and comprehensive use of resources [21].

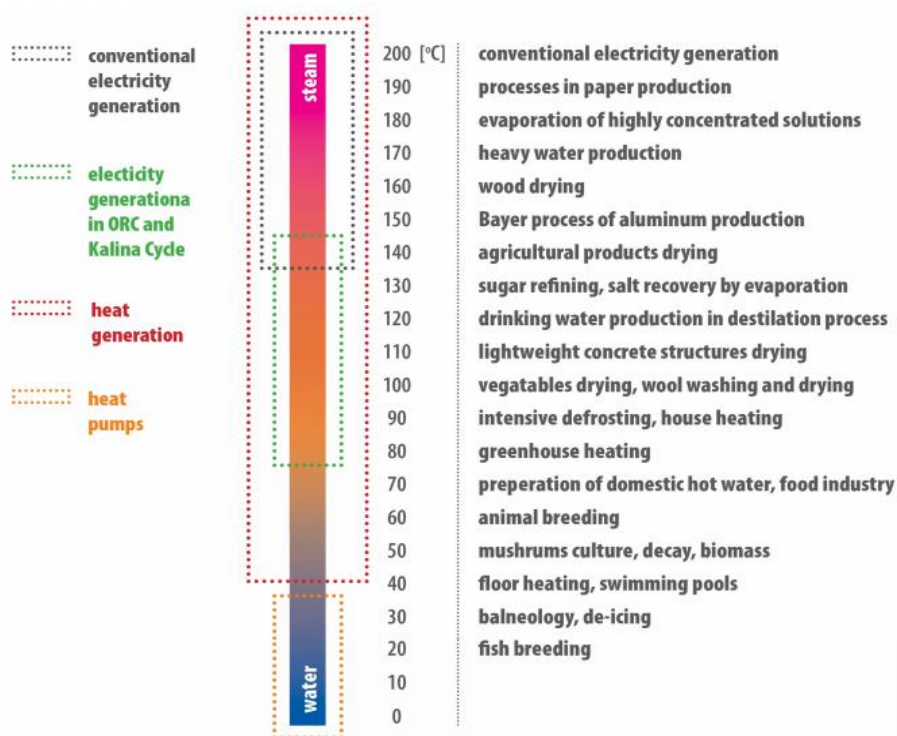


FIGURE 7: MODIFIED LINDAL DIAGRAM (BASED ON [22,23])

## 1.8 Geothermal Power plants

Geothermal power plants are classified into two types: steam and binary power cycles. The steam power cycle is mostly utilised for high enthalpy fluids, whereas binary plants are used for low or medium enthalpy fluids.

### Single flash steam power plant:

The schematic diagram of the single flash steam power plant is shown in Figure 8. Due to the low steam quality that emerges from the two-phase fluid following the expansion valve, the employment of a flash system results in the removal of a substantial percentage of energy in brine (liquid) form from the separator. Single flash power plants are often regarded as the most cost-effective option for accessible geothermal resources with temperatures exceeding 190 °C. For natural pressure circumstances, higher temperature resources will generate more liquid and steam. For high-temperature resources dominated by two phases, the geothermal fluid is transported to the borehole's surface as a combination of steam and liquid (brine). Steam separation from brine takes place in either a horizontal separator under gravity influence or a vertical separator under cyclonic motion. The steam is then sent to the steam turbine, while the saturated liquid is used as a heat input source for ORC in a combined flash-ORC power plant [24], or the steam is re-injected into the reservoir through a re-injection well [26].

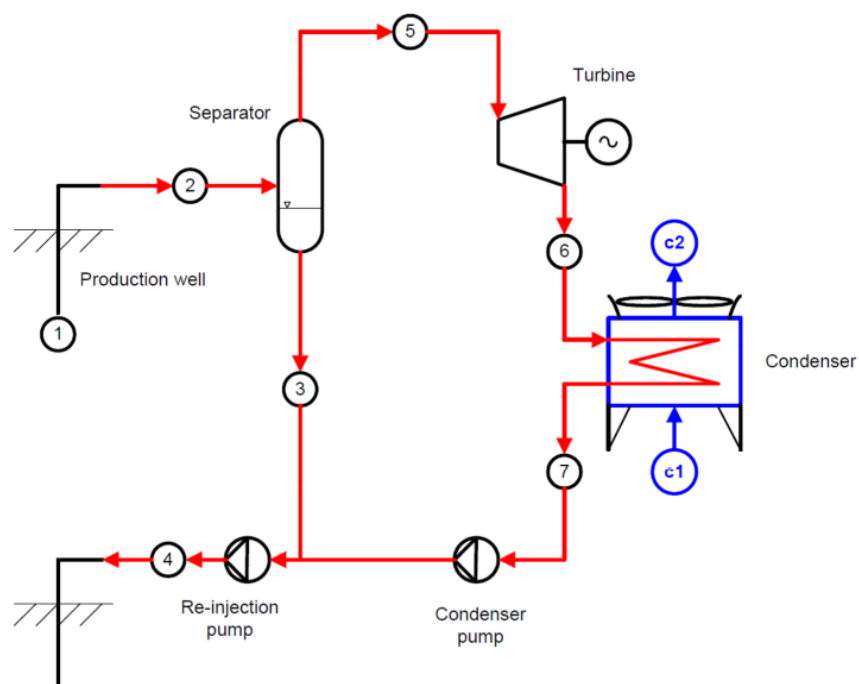


FIGURE 8: SINGLE FLASH POWER PLANT [25]

### Dual Flash steam power plant:

Depending on the resource circumstances, the dual flash steam plant (double flash) is chosen above the single flash steam power plant. In actuality, it is identical to a single flash power plant, except that it generates more steam since it employs two separators. Figure 9 depicts a schematic representation of a twin flash power plant. When two separators are used, a two-stage steam turbine is used, with one stage operating at high pressure and the other at low pressure.

Dual flash power plants may create up to 15%–25% more electricity than a single flash power plant since their power output capacity ranges from 4.7 MW to 110 MW. In a dual flash power plant, the saturated liquid exiting the first separator is routed to a lower pressure second separator, resulting in increased steam output. Following the generation of steam at high and low pressures, all steam is sent to a steam turbine through separate pipes. The steam turbine might be a dual admission turbine, a distinct turbine, or a combination of two independent tandem compound turbines that function based on the inlet pressure of the steam. A twin flash power plant's components are identical to those of a single flash steam power plant. The mineral content of the water becomes concentrated depending on how the dual flash is designed, hence the resource conditions are of extreme importance [26].

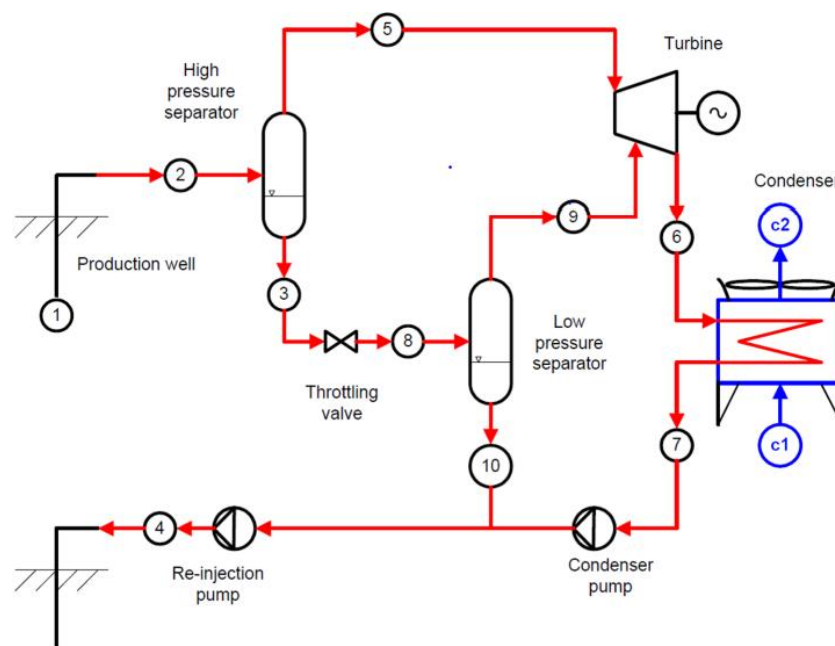


FIGURE 9: DUAL FLASH POWER PLANT [25]

### Binary Power Plant:

Instead of water, a secondary fluid such as hydrocarbon or fluorocarbon is utilised to power the ORC turbine in this type of power plant. The geothermal fluid is circulated in a vaporizer and returned to the re-injection well at ORC. The heat exchange between the geothermal fluid and the secondary fluid heats and vaporises the secondary fluid in the vaporizer. The vapour produced by the secondary fluid is sent to the turbine, which generates power. The vapour from the turbine is routed to a regenerator, where the superheated steam is utilised

to heat the condensed fluid exiting the condenser before entering the vaporizer. The schematic diagram of ORC power plant is shown in Figure 10.

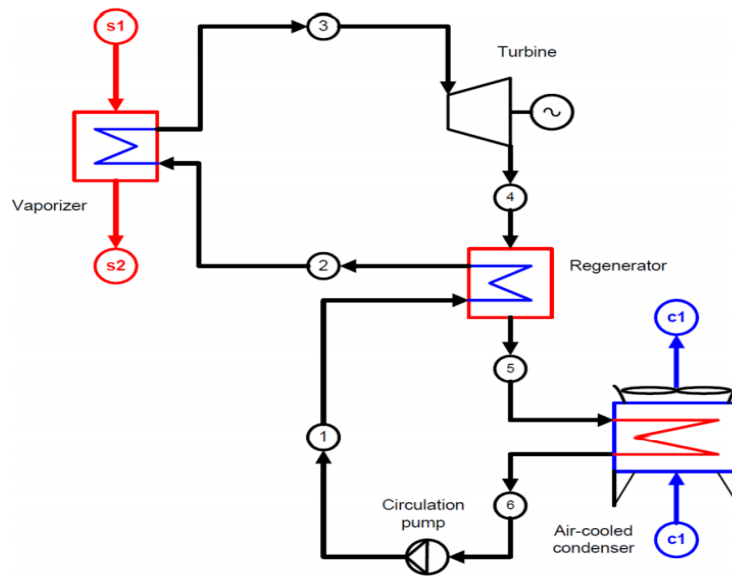


FIGURE 10: BINARY FLASH POWER PLANT [25]

The primary benefits of ORC are that it works at a low temperature, resulting in minimal mechanical loads on the turbine, and that there is no erosion of the turbine blades owing to the absence of moisture during the vapour expansion in the turbine. Furthermore, because the turbine in ORC is smaller in size, it is less costly, and there are no difficulties with air in-leakage or problems caused by working in a vacuum, because a vacuum is not required [27].

## 2. MATERIALS AND METHODS

### 2.1 Coaxial borehole heat exchanger

For heat extraction, we explored a co-axial pipe design in our thesis study. Fluids are cycled in the borehole, where they are not in touch with the surrounding formation, in the single-well (closed-loop) ideas. Despite the much-reduced contact area achieved by fracturing, it is anticipated that adequate heat may be transmitted from the formation to the wellbore. To decrease heat transmission between the fluid in the tubing and the fluid in the annulus, the tubing is always thermally insulated. At the wellhead, return fluid will be collected, and heat will be recovered and used for various reasons. These solutions may be more appealing due to decreased geological/reservoir risk (no direct fluid-rock interaction) and cheaper cost (one well only).

When discussing the hazards of an enhanced geothermal system, we must consider the requirement for a production well and an injection well. Reinjection operations have significant economic expenses since they necessitate the drilling and maintenance of additional wells, as well as the treatment and pumping of fluids. Reinjection carries some risks as well: the injected cold water may interfere with the hot waters of the production level, often due to "short-circuiting" along direct flow-paths such as open fractures; geothermal fluids may pollute groundwater; corrosion and scaling in surface pipelines and reinjection wells; and seismicity.

Recent research has begun to shift focus to double pipe heat exchangers due to the advantages of double pipe in heat exchange efficiency, pumping energy savings, and reduced grout consumption. Double pipe heat exchangers have a bigger surface area to exchange heat and a larger volume of fluid to exchange heat than u-tube heat exchangers. Fluid flow velocity with double pipe geometry may be lower at the same injection rate, requiring less hydraulic pressure to circulate the fluid, resulting in lower pumping energy consumption. Furthermore, in cased abandoned wells, installing a double pipe heat exchanger is a better alternative than U-tube since the outer pipe (casing) is already existent, saving money and time; however, most existing casings are not in a state that allows them to be used in this manner. Finally, the coaxial design of a double pipe heat exchanger reduces thermal resistance between the flowing fluid and the wellbore.

The borehole that surrounds the pipes is backfilled with a material that has a high thermal conductivity. The injected water absorbs heat from the surrounding rock formations, heats up, and eventually returns to the surface - the medium's circulation is depicted schematically in Figure 11 [28]. The figure depicts the WBHX's schematic layout as well as a cross-section. The well bottom will be sealed, and a double shell co-axial tube will be installed. In the annular area between the well casing and the exterior shell, the heat carrier fluid enters the wellbore heat exchanger. The fluid absorbs heat from the surrounding earth as it flows downward. The fluid is directed upward at the bottom end and flows into the internal pipe up to the wellhead. To decrease heat exchange between upward and downward flow, the space between the two pipes is covered with insulating material.

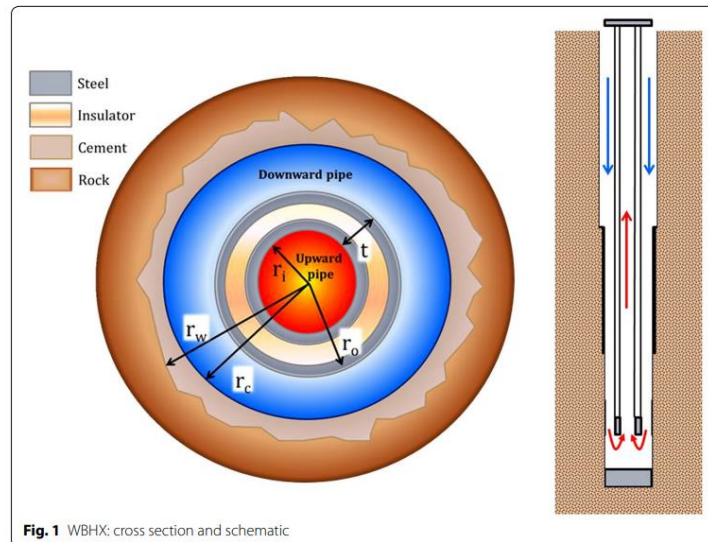


FIGURE 11: CO-AXIAL BOREHOLE HEAT EXCHANGER [28]

In general, the deeper the BHE, the greater the heat transfer area, the higher the temperature of the surrounding rock, and the higher the heat conductivity. Thus, deep borehole heat exchangers (DBHEs) can achieve greater output temperatures by converting dry unsuccessful or existing unexploited hydrocarbon wells.

The deep borehole heat exchanger's primary drawback is its poor heat recovery efficiency when compared to traditional geothermal technology. This is owing to the reduced mass flow rate and indirect heat exchange, which results in a lower wellhead temperature. However, using a WBHX might be a solution for extracting heat from unusual geothermal systems, such as magmatic or hypersaline reservoirs, where fluids with certain physical and chemical properties exist. The manufacturing of such fluids entails considerable technological challenges as well as high economic expenses, which might result in a non-profitable investment. The WBHX could be also an alternative to hydrofracking methods to exploit the hot dry rock reservoirs [28].

## 2.2 Wells Description

The well's characteristics were derived from the Italian National Geothermal Database (GEOTHOPICA), which was created in 1993 by the International Institute of Geothermal Research Council [29]. For our thesis study, we chose two hydrocarbon wells in northern Italy. Among the information gathered from the database are:

- Identification and location of the wells,
- Temperature and depth,
- Temperature gradient and heat flow,
- Litho-stratigraphic column of the wells.

The two Selected wells for our thesis work are as follows:

- 1) CASTEGGIO 2
- 2) TURBIGO 1



## CASTEGGIO 2

This well is in the Lombardia, province of Pavia. It is an exploratory hydrocarbon well. The well has a depth of 2501 metres and is split into three stratigraphic strata (figure 12) with a geothermal gradient of 0.025 °C/km (Figure 13). The location and the rock lithology and properties of the well are reported in Table 2 & 3.

**TABLE 2: CASTEGGIO DESCRIPTION**

Name	Lat(ggppss)	Lon(ggppss)	Depth(m)	Type of well
Casteggio	450100	90610	2501	Production well
Purpose	Lon(gg.ddddddd)		Lat(gg.ddddddd)	
Hydrocarbon	9.1027777778		45.01666666667	

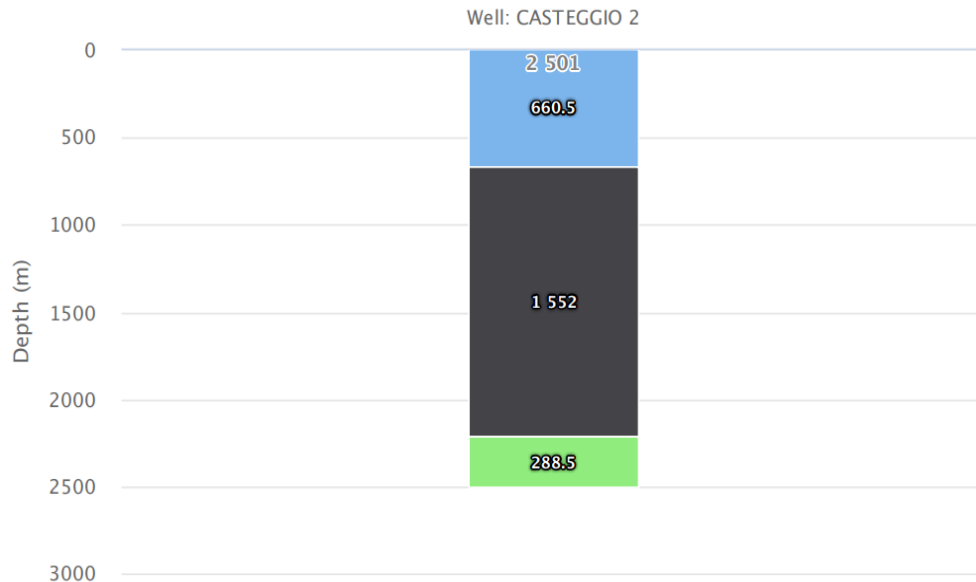


**FIGURE 12: LITHO-STRATIGRAPHIC PROFILE OF CASTEGGIO (DATA DERIVED FROM THE ITALIAN NATIONAL GEOTHERMAL DATABASE)**

**TABLE 3: LITHO-STRATIGRAPHIC DATA OF CASTEGGIO [37]**

Depth (m)	Lithology	Age	Thermal Conductivity (W/m.K)	Heat Capacity (J/kg.K)	Density (kg/m <sup>3</sup> )
0 - 660.5	Sands and Clays	Quaternary	2.45	1459	1757
660.5 – 2212.5	Clays and Sandy marls	Pliocene	3.28	1125	2161
2212.5 - 2501	Marls, sands and gravels	Miocene	2.77	733	1787

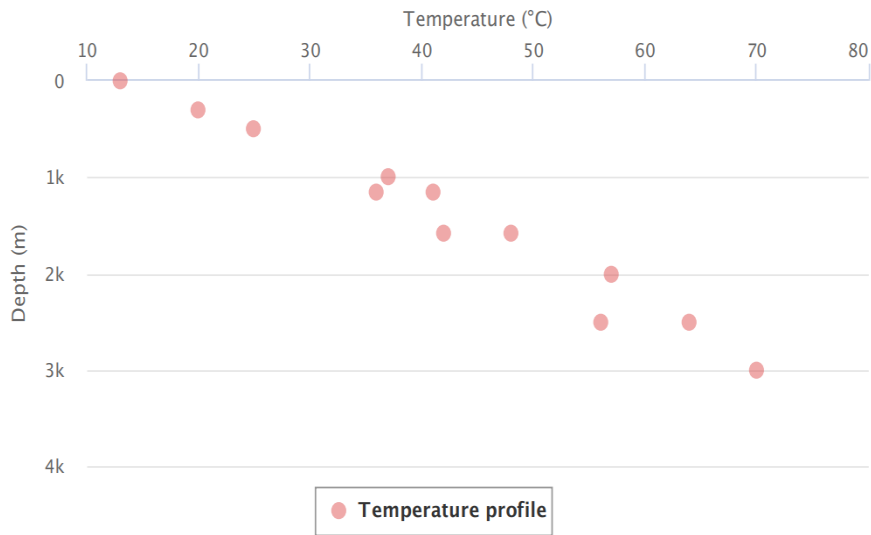


**FIGURE 13: TEMPERATURE PROFILE OF CASTEGGIO (DATA DERIVED FROM THE ITALIAN NATIONAL GEOTHERMAL DATABASE)**

### TURBIGO 1

It is located approximately 35 kilometres (22 miles) west of Milan in the Province of Milan in the Italian region Lombardy. It is a hydrocarbon exploration well. The well has a depth of 6632.7 metres and is split into eight stratigraphic strata (Figure 14) with a geothermal gradient of 27°C/km (Figure 15). The location and the rock lithology and properties are reported in Table 4 & 5.

**TABLE 4: TURBIGO DESCRIPTION**

Name	Lat(ggppss)	Lon(ggppss)	Depth(m)	Type of well
Turbigo	453128	84601	6632.7	Exploration well
<b>Purpose</b>	<b>Lon(gg.dddddd)</b>		<b>Lat(gg.dddddd)</b>	
Hydrocarbon	8.76694444		45.52444444	

## Litho-Stratigraphic profile

Italian National Geothermal Database 2.0

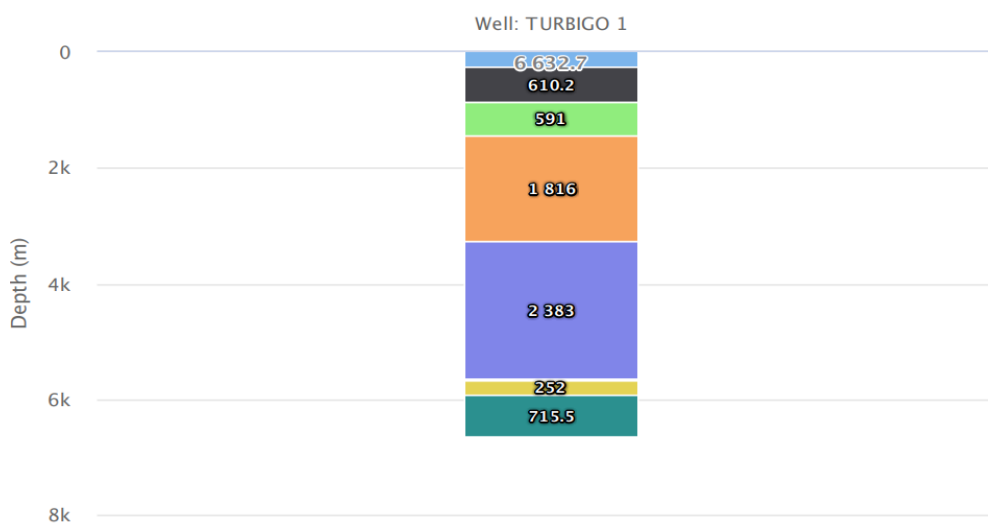
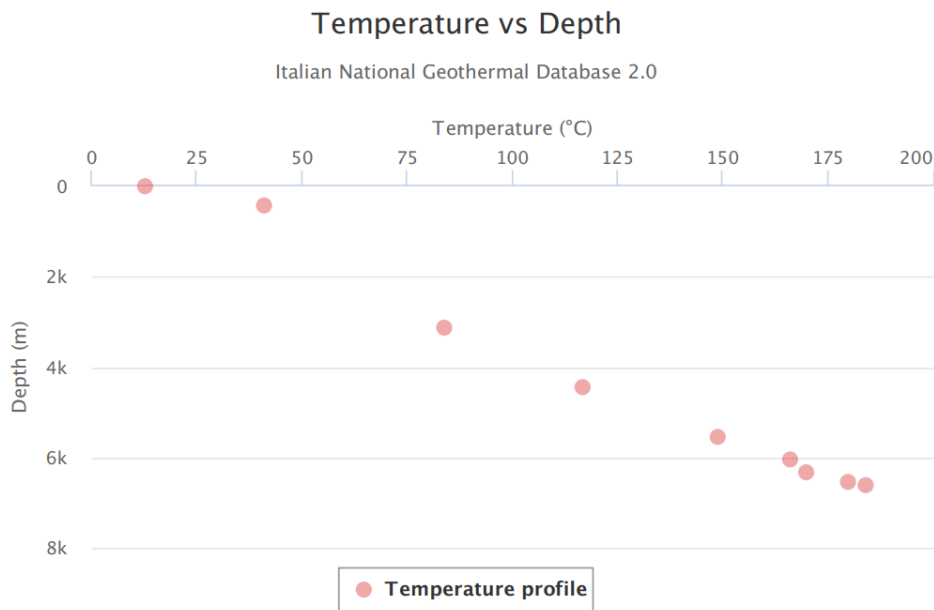


FIGURE 14: LITHO-STRATIGRAPHIC PROFILE OF TURBIGO (DATA DERIVED FROM THE ITALIAN NATIONAL GEOTHERMAL DATABASE)

TABLE 5: LITHO-STRATIGRAPHIC DATA OF TURBIGO [37-44]

Depth (m)	Lithology	Age	Thermal Conductivity (W/m.K)	Heat Capacity (J/kg.K)	Density (kg/m <sup>3</sup> )
0 – 610.2	Sands, pebbles and clays	Quaternary	2.45	1459	1757
610.2 – 1201.2	Clays, sand and pebbles	Pliocene	2.45	1459	1757
1201.2–3017.2	sand and clays	Miocene	2.45	1459	1757
3017.2-5400.2	Clay, sandstones, conglomerates	Oligocene	2.06	770	2640
5400.2-5421.2	Marls and limestone	Eocene	2.72	680	2720
5421.2-5665.2	Marls, sandstone and limestones	Cretaceous	2.15	680	2640
5665.2-5917.2	Marls, limestone, dolomite and selce	Jurassic	2.24	900	2720
5917.2-6632.7	Limestone, dolomite, marls, clays and sand	Triassic	2.5	860	2680



**FIGURE 15: TEMPERATURE PROFILE OF TURBIGO (DATA DERIVED FROM THE ITALIAN NATIONAL GEOTHERMAL DATABASE)**

### **2.3 Analytical models**

Modelling is an important field of study and has been a key tool for system optimization, long-term efficiency testing, and determining the effective thermal conductivity of rocks. In order to evaluate the economic and environmental advantages of these systems, certain thorough simulations are also required. Costs and losses increase when a system is large or has an inadequate number of exchangers. As a result, the development of an effective, dependable, and precise calculating tool is necessary. Existing models can be classified as analytical or numerical, and then further classified as global or local. Heat and mass transfer occur in the ground and exchanger in global models, whereas heat and mass transport occurs within the heat exchanger in local models.

There are currently several models available to assist in determining transient heat transfer in the Ground heat exchanger. Many theoretical models have been developed based on the analytical solutions offered by classical models such as the line source model and the cylindrical source model.

#### **Line Source Model (LSM):**

The Line Source Model was the first method used to calculate thermal transport around a heat exchange pipe in the ground. The LSM model assumes that:

- the source borehole heat exchanger is an infinite source with constant power,
- the rock mass is an infinite medium with uniform initial temperature,
- heat transfer in the direction of the borehole axis is ignored, including heat flux across the ground surface and down the borehole's bottom, and
- the heat conduction process in the ground is simplified as one-dimensional.

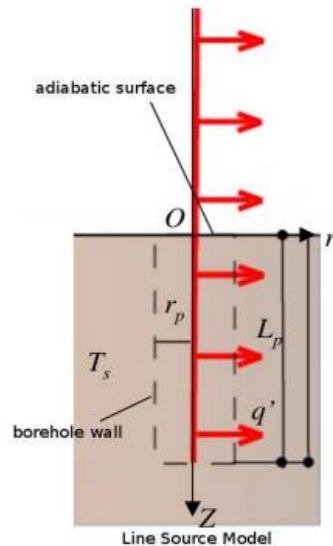


FIGURE 16: SCHEMATIC OF LINE SOURCE MODEL

The equation for the temperature field as a function of time (t) and radius (r) around a line source with constant heat injection rate (q) describe

$$T(r, t) - T_0 = \frac{ql}{4\pi\lambda} \left( \ln \left( \frac{4at}{r^2} \right) - \gamma \right) \quad (1)$$

$\gamma = 0.5772\dots$  is Euler's constant. The maximum error is 2.5% for  $at/r^2 \geq 20$  and 10% for  $at/r^2 \geq 5$ .

The drawback of this approach is that it ignores the impacts of borehole heat exchange. Only heat conduction in the radial direction was anticipated. The interior structure of the borehole is the model's next approximation (Figure 16). It was used the general heat transfer coefficient, which is typical for heat resistance in both rocks and boreholes. The line source concept is based on heat exchange with a continuous heat flow. The average heat flow throughout each month is considered for the modelling of heat transfer in the heat exchanger as a function of time [30].

The model is presented by Hart and Couvillion [31], who employ the notion of continuous heat transfer between the rock mass and the line source. As a result of the model, they were able to determine the temperature distribution around the line source as a function of operating time. A superposition of solutions from a single borehole is used to represent the effect of thermal interference between the boreholes. However, this model has the same constraints as the line source model. Despite the aforementioned critiques of the line source model, this approach was frequently employed to evaluate the thermal conductivity of the rock mass, often known as the "thermal response test (TRT)."

#### Cylindrical Source Model:

Carslaw and Jaeger [32] used the cylindrical source model to represent a borehole as an infinite cylinder surrounded by a homogenous substance with stable characteristics. Heat flux was applied directly to the surface of the borehole cylinder, which meant that the heat

capacity of the U-tube and grout could be completely ignored. This is referred to as a "hollow" model (see fig. 17). The temperature field equation as a function of time (t) and radius (r), assuming a cylindrical source with constant power, as illustrated in (2). [30]

$$\theta(r, t) = \frac{ql}{\pi^2 \lambda r_b} \cdot \left[ \int_0^\infty \left( e^{-au^2t} - 1 \right) \frac{J_0(ur)Y_1(ur_b) - Y_0(ur)J_1(ur_b)}{u^2 [J_1^2(ur_b) + Y_1^2(ur_b)]} du \right] \quad (2)$$

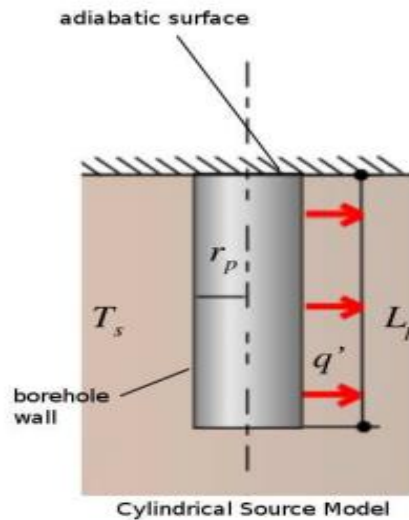


FIGURE 17: SCHEMATIC OF CYLINDRICAL SOURCE MODEL

where:  $J_0, J_1, Y_0, Y_1$  - Bessel functions

$\theta = T - T_0$

$ql$  - heat source.

Kavanaugh presents a model to calculate the temperature in the ground or the intensity of heat transmission based on the theory of the cylindrical source model. This model also makes certain assumptions. Because rock mass is a homogenous infinite media, it is assumed that the borehole walls have a constant surface temperature or that there is a continuous heat flow of heat exchange between the rock mass and the borehole wall. It is also believed that the heat exchange between the fluid and the rock mass occurs by pure conduction, without taking into consideration heat transfer, which is affected by the fluid's flow rate.

#### Eskilson's Model:

Both the one-dimensional Kelvin's theory model and the cylindrical source model ignore the axial heat flow throughout the borehole depth, making them unsuitable for long-term operation of these systems. Eskilson (1987) made significant progress in accounting for the finite length of the borehole [33]. According to the Eskilson model:

- the ground is assumed to be homogeneous with constant initial and boundary temperatures,
- and the thermal capacitance of the borehole elements such as the pipe wall and the grout are neglected.

The basic formulation of the ground temperature is governed by the heat conduction equation in cylindrical coordinates:

$$\begin{aligned} \frac{\partial^2 T}{\partial r^2} + \frac{1}{r} \frac{\partial T}{\partial r} + \frac{\partial^2 T}{\partial z^2} &= \frac{1}{a} \frac{\partial T}{\partial t} \\ T(r, 0, t) &= T_0 \\ T(r, z, 0) &= T_0 \\ q_l &= \frac{1}{H} \int_D^{D+H} 2\pi r \lambda \left. \frac{\partial T}{\partial r} \right|_{r=r_b} dz \end{aligned} \quad (3)$$

where: H - borehole length,

D - means the uppermost part of the borehole, which can be thermally neglected in engineering practice.

The numerical finite-difference approach is utilised on a radial-axial coordinate system in the Eskilson model to get the temperature distribution of a single borehole of finite length. The ultimate expression of the temperature response at the borehole wall to a unit step heat pulse is a function of  $t/t_s$  and  $r_b/H$ , known as the "g-function": where H is the borehole length and D is the topmost section of the borehole, which may be thermally ignored in engineering practise. In Eskilson model, the numerical finite-difference method is used on a radial-axial coordinate system to obtain the temperature distribution of a single borehole with finite length. The final expression of the temperature response at the borehole wall to a unit step heat pulse is a function of  $t/t_s$  and  $r_b/H$  so called "g-function":

$$T_b - T_0 = -\frac{q_l}{2\pi\lambda} g\left(\frac{t}{t_s}, \frac{r_b}{H}\right) \quad (4)$$

$t_s = H^2/9a$  - means the steady-state time.

The dimensionless temperature response at the borehole wall, calculated numerically, is the g-function. Another significant accomplishment of Eskilson's model is the use of special superimposition to account for the temperature responses of numerous boreholes. Furthermore, the sequential temporal superimposition method was utilised to compute the temperature response (i.e., g-functions) to any arbitrary heat rejection/extraction that can be broken into a sequence of single pulses. In other words, the particular and temporal superimpositions can influence the total temperature response of the GHE to any heat rejection/extraction at any moment. However, this technique is time-consuming, and it cannot be immediately integrated into a design and energy analysis software for practical applications since the g-functions of the GHEs with different configurations must be pre-computed and saved in the computer as a huge database [34].

### Finite line-Source Solution:

An analytical solution to the finite line source has been found based on Eskilson's model. This model takes into account the influences of the borehole's finite length and the ground surface as a boundary and assumes that: the ground is a homogeneous semi-infinite medium with constant thermophysical properties, the medium's boundary, i.e., the ground surface, maintains a constant temperature, the same as its initial temperature throughout the period concerned, and the radial dimension of the borehole is neglected so that it may be approximated as a line-source stretching from the boundary to a certain depth,  $H$ , the heating rate per length of the source,  $ql$ , is constant since the starting instant  $t = 0$ .

The equation for the temperature distribution in the rock mass present

$$T(r, z, t) - T_0 = \frac{ql}{4\pi\lambda} \cdot \int_0^H \left[ \frac{\operatorname{erfc}\left(\frac{r^2+(z-h)^2}{2\sqrt{at}}\right)}{\sqrt{r^2+(z-h)^2}} - \frac{\operatorname{erfc}\left(\frac{r^2+(z+h)^2}{2\sqrt{at}}\right)}{\sqrt{r^2+(z+h)^2}} \right] dh \quad (5)$$

It can be seen from (5) that the temperature on the borehole wall, where  $r = r_b$  varies with time and borehole depth. The temperature at the middle of the borehole depth ( $z = 0.5H$ ) is usually chosen as its representative temperature. An alternative is the integral mean temperature along with the borehole depth, which may be determined by numerical integration of (5). The integral of (5) can be computed much faster than the numerical solution of the same heat conduction problem in the semi-infinite domain with a long duration. When described in the preceding section, as the time approaches infinity, the temperature rises of Kelvin's theory approaches infinity, but the temperature from the finite line-source model approaches the steady state, which corresponds to the real heat transfer process. In the case of long duration, there may be a significant difference between Kelvin's model and the finite line source [34].

All of the given analytical models are global models in which heat transmission is concerned around the heat exchanger rather than within it. This method greatly lowers calculation time; nevertheless, it is insufficiently precise since it does not fully account for the number of phenomena occurring within the heat exchanger.

#### **2.4 Heat transfer model used in our thesis work**

Conduction and convection are used to transfer heat between heated rock and water flowing in a deep borehole heat exchanger. The model in the paper (Alimonti and Soldo 2016) was created using an analytical solution of the Fourier equation and implemented in a C computation code. The model's equations are presented in the following paragraphs. The coaxial borehole heat exchanger is explored in this study. The fluid flows downward through the outer pipe and upward through the inner pipe. Figure 18 depicts the schematic heat transfer process in a coaxial heat exchanger.



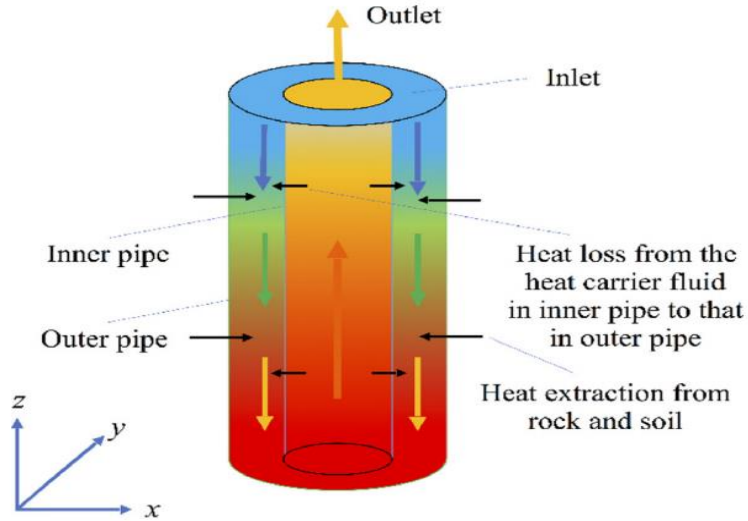


FIGURE 18: SCHEMATIC REPRESENTATION OF HEAT TRANSFER IN CO-AXIAL HEAT EXCHANGERS [35]

### Temperature of formation rocks

Using a ground surface temperature  $T_0$  of 25 °C, the rock temperature at the depth 'z' has been evaluated using the following relation:

$$T_w(z) = T_0 + GT \cdot z \quad (6)$$

Where GT is the geothermal gradient of the site.

### Heat transfer in the downward pipe

The heat transfer from the rock in the model is mostly due to conduction; no convection occurs. The heat is then transferred by conduction from the reservoir to the WBHX's exterior casing, which is protected from the rock wall by a layer of cement. Convection occurs in the borehole heat exchanger during the heat transfer between the casing and the water.

The heat acquired by the water in the downward pipe is directly proportional to the length of the pipe ( $\Delta z$ ), the external radius of the borehole ( $r_w$ ), the total heat exchange coefficient ( $k_t$ ), the difference between the rock temperature at depth z ( $T_w$ ) and the temperature of the fluid in the outer pipe ( $T_{f,down}$ ). The thermal power can be calculated with the following relation [28]:

$$Q_{down} = 2\pi r_w k_t (T_w(z) - (T_{f,down})) \Delta z \quad (7)$$

The total heat transfer coefficient is the reciprocal of the total thermal resistance, which can be calculated as:

$$R_t = R_a + R_c + R_s \quad (8)$$

The three terms in Eq. (3) are the thermal resistance due to the convection into the annular space of the WBHX ( $R_a$ ), the thermal resistance due to the conduction through the casings ( $R_c$ ); the thermal resistance due to the conduction in the rock ( $R_s$ ).

To evaluate the conductive thermal resistance in the rock the thermal conductivity of the rock  $\lambda_s$ , the thermal diffusivity of the rock  $a_s$ , the external radius of the well  $r_w$ , and the elapsed time since the start  $t'$  must be known:

$$R_s = \frac{1}{2\lambda_s} \ln \frac{2\sqrt{a_s t'}}{r_w} \quad (9)$$

This equation arises from the analytical solution of heat transfer equation given in Carslaw and Jaeger (1959). The term  $2\sqrt{a_s t'}$  represents the travelling distance of the temperature front. At distance  $> 2\sqrt{a_s t'}$  in the rock the temperature is undisturbed and equal to  $T_w$ .

To evaluate the thermal resistance ' $R_a$ ' the radius of the external casing ' $r_c$ ' and the convective heat transfer coefficient ' $h$ ' must be known:

$$R_a = \frac{1}{2.r_c.h} \quad (10)$$

The convective heat transfer coefficient is calculated using the definition of the Nusselt number,  $Nu$

$$h = Nu. \frac{\lambda_f}{2.r_c} \quad (11)$$

and by a form of Dittus-Boelter equation, having assumed turbulent flow inside the tubes

$$Nu = 0.023. Re^{0.8}. Pr^{0.4} \quad (12)$$

The exponent of the Prandtl number varies somewhat among studies and is affected by the correlation utilised. Different formulas can also be employed to determine the Nusselt number at the shell side, although the potential influence on the heat transfer coefficient is irrelevant for the values investigated.

Thus, the convective heat transfer coefficient can be calculated as:

$$h = \frac{0.023.\lambda_f.Re^{0.8}Pr^{0.4}}{2.r_c} \quad (13)$$

The thermal resistance to heat conduction through the casings of the well completion is determined as:

$$R_c = \sum_{i=1}^n R_{\lambda i} = \frac{1}{2} \sum_{i=1}^n \frac{1}{\lambda_i} \ln \frac{r_{c,i+1}}{r_{c,i}} \quad (14)$$

Where,  $\lambda_i$  = thermal conductivity of  $i$ th casing layer.

The impact of the cementing ring was investigated by determining the mutual thermal resistance (to heat conduction) of the concrete and rock. The results reveal that, despite the fact that the thermal conductivity of the concrete is lower than that of the rock, the presence of cement is minimal due to the small thickness of the grouting layer in relation to the extension of the rock.

The total heat exchange coefficient can be calculated as:

$$\frac{1}{k_t} = \frac{D_c}{2 \cdot \lambda_s} \cdot \ln \frac{4\sqrt{a_s t'}}{D_c} + \frac{1}{h} \quad (15)$$

### Heat transfer in the upward pipe:

The water after collecting heat from the rocks enters in the inner pipe and exchange heat with the wall of composite pipe. The thermal power can be calculated as:

$$Q_{up} = 2\pi r_i k_o (T_{f,up} - T_{f,down}) \Delta z \quad (16)$$

Where,

$r_i$  = radius of the inner tube,

$k_o$  = the overall heat transfer coefficient

$T_{f,up}$  = the temperature of the water in the inner pipe

$T_{f,down}$  = the temperature of the fluid in the outer pipe.

$\Delta z$  = the length of the pipe.

Using the theory of the heat exchange in the multi-layer cylindrical wall, the total heat exchange coefficient  $k_o$  can be calculated with the relation:

$$\frac{1}{k_o} = \frac{r_i}{r_i+t} \cdot \frac{1}{h_o} + r_i \sum_{i=1}^n \ln \left( \frac{r_{j+1}}{r_j} \right) \cdot \frac{1}{\lambda_j} + \frac{1}{h_i} \quad (17)$$

The first element in Eq. (17) is caused by convective heat transmission to the outer wall: ' $r_i$ ' is the radius of the inner tube, ' $t$ ' is the thickness of the composite pipe, and ' $h_o$ ' is the convective heat transfer coefficient to the outside wall. The second factor in Eq. (17) is linked to conductive heat transmission through the composite pipe: ' $\lambda_j$ ', ' $r_j$ ' are the material's thermal conductivity and radius, respectively (air and steel). The third component of Eq. (17) is caused by convection to the inner wall.

### The thermo-siphon effect

The WBHX has been designed to create the most thermal power while utilising the least amount of electrical energy to push the fluid down the pipe. This state is accomplished by spontaneous circulation caused by the thermo-siphon effect: as the fluid is heated, it naturally returns to the top via the inner tube. The pressure increase is caused by a difference in density, which is lower in the descending pipe than in the upward pipe (Add reference).

$$\Delta P = \rho \cdot g \cdot z - \Delta P_f \text{ downward} \quad (18)$$

$$\Delta P = -\rho \cdot g \cdot z - \Delta P_f \text{ upward} \quad (19)$$

$$\Delta P_f = f \frac{\Delta z}{D} \rho(T) \frac{v^2}{2} \quad (20)$$

where  $\Delta P_f$  are the friction losses,  $f$  is the friction factor calculated with the explicit correlation of Churchill (1977),  $\Delta z$  and  $D$ , are respectively the length and the diameter of the pipe, ' $\rho$ ' and ' $v$ ' are, respectively the density and the velocity of the fluid.

Considering that the pipes are very large in length, the hypothesis of none local pressure losses has been used.

### **Accumulated Heat Energy**

For estimation of heat energy  $Q$  gained by the circulating fluid due to temperature differences, the following equation is used [36]:

$$Q = m \cdot C_p \cdot \Delta T = m C_p (T_{out} - T_{in}) \quad (21)$$

where  $m$  is the fluid mass,  $T_{in}$  is the inlet temperature of working fluid injected to the annulus,  $T_{out}$  is the outlet temperature of working fluid circulated out of the geo-string, and  $\Delta T$  is the temperature difference between the outlet temperature and the inlet temperature.

### 3. RESULTS & DISCUSSIONS

We used the methodologies and equations mentioned above for WBHX analysis to get maximum heat at the surface for two wells in northern Italy by changing technical factors as well as physio-chemical characteristics of rocks. The litho-stratigraphic information is derived from the Italian National Geothermal database.

To examine the effect of each parameter on the fluid's outlet temperature and thermal heat, we maintained everything constant while altering only one parameter to see which value yielded the highest outlet temperature and thermal heat. This method is sometimes referred to as sensitivity analysis. The following characteristics have a significant impact on the efficiency of heat extraction from the well.

#### CASTEGGIO 2

##### Impact of inlet flow rate of the working fluid

Analyzing the findings in both examples, A and B, we can conclude that a flowrate of 0.5 – 0.8 kg/s yields a greater value of outlet temperature than a flowrate of 3 kg/s, which yields a lower value of fluid outlet temperature. When the flowrate is increased, the fluid comes into contact with the rock formation for a shorter period of time while moving downward and is unable to extract an adequate quantity of heat from the formations. When the flow rate is increased, the returning fluid loses less heat. Because of the greater flowrate, the red line in Figure 19 becomes straight. The red line in Figure 20, on the other hand, indicates the steady fall in temperature as the fluid reaches the surface due to heat loss with the fluid moving in the outer pipe.

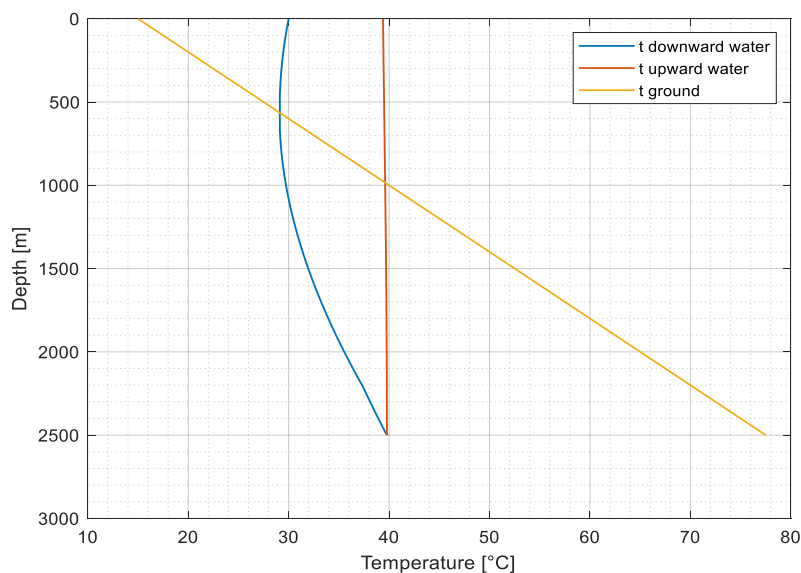


FIGURE 19: CASE A- INLET FLOWRATE = 3 KG/S, OUTLET TEMP = 39.5°C, INLET TEMP = 30°C

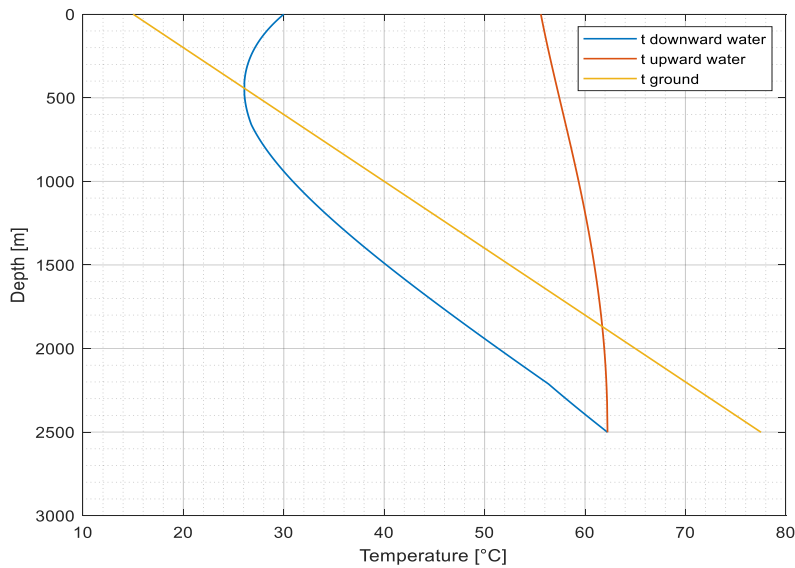


FIGURE 20: CASE B- INLET FLOWRATE = 0.5 KG/S, OUTLET TEMP = 55.8°C, INLET TEMP = 30°C

It is apparent that as the inlet flow rates increase, so does the temperature at the bottom. At low injecting flow rates, the fluid temperature in the inner pipe falls fast from the bottom to the exit. This is mostly due to the fact that the low-speed water in the outside pipe has sufficient time to absorb heat from the earth, resulting in a high temperature of the bottom fluid. When the fluid in the inner pipe travels upward, the heat absorbed is transferred to the fluid in the outer pipe due to the large temperature differential between the fluids in the inner and outer pipes and the long-term heat exchange.

The output temperature decreases from 55.8 °C to 39.5 °C with an increased injection rate from 0.5 kgs to 3 kg/s. However, the geothermal power mainly depends upon the inlet flowrate of the circulating fluid since increasing the flowrate increases the heat power. So, the geothermal power well increases from 54.38 to 120.142 kW. Figure 21 shows the variation in outlet temperature as the inlet flowrate changes.

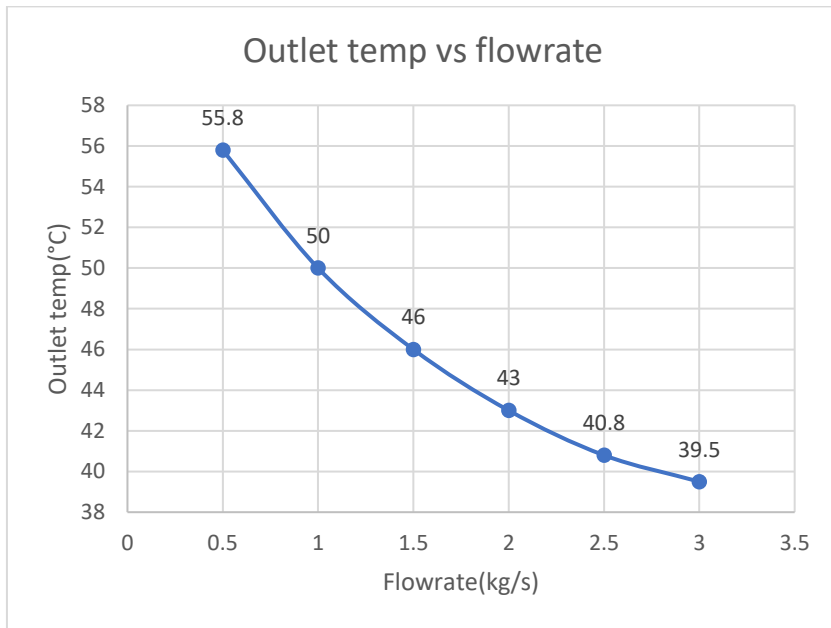


FIGURE 21: VARIATION IN OUTLET TEMP AS INLET FLOWRATE CHANGES

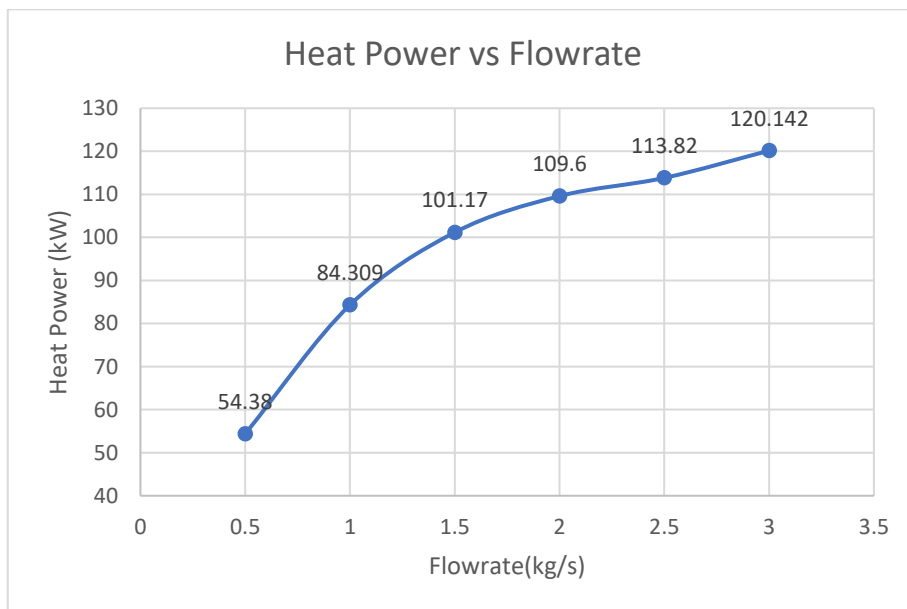


FIGURE 22: HEAT POWER VS INLET FLUID RATE

The rise in heat power as the flowrate increases is seen in Figure 22. The heat power is proportional to the flowrate of the injected fluid and is calculated using equation (21). However, raising the flowrate may result in greater values of thermal power, but it may increase the cost of the system since we may require pumping power to circulate the fluid through the pipe.

Inlet temperature of working fluid

The temperature of the inlet fluid is an essential design parameter that affects the thermal performance of a wellbore heat exchanger. The thermal performance of WBHX has been

examined in this section for a variety of inlet temperature ranges. The temperature of the injected fluid is adjusted between 30 to 60°C. The injecting fluid flowrate was kept constant throughout the study, at 3 kg/s.

Figure 26 depicts the outlet temperature for various inlet water temperatures, and it is discovered that as the inlet temperature rises, the output temperature climbs linearly. Figures 23, 24 & 25 demonstrate that for every 10 degrees increase in intake water temperature, the output temperature rises by 4.5°C to 5°C.

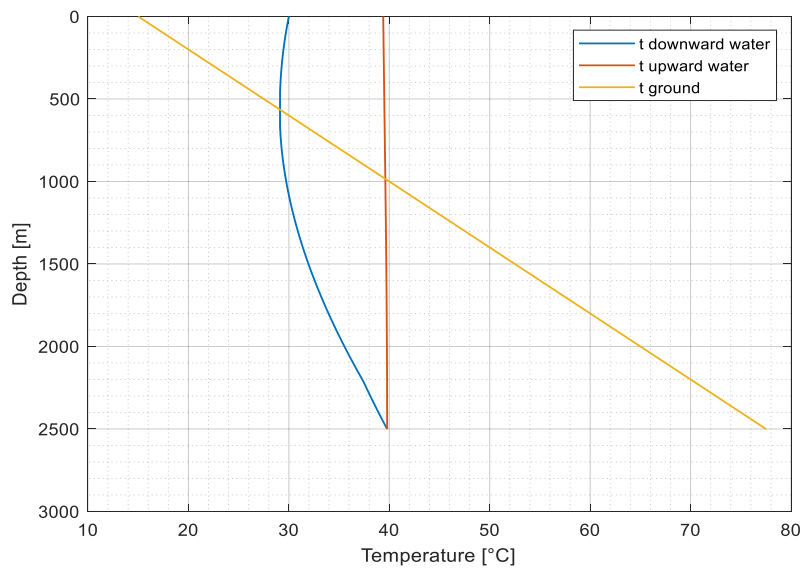


**FIGURE 23: CASE A-  $T_{INLET} = 30^{\circ}\text{C}$ ,  $T_{OUTLET} = 39.5^{\circ}\text{C}$ , FLOWRATE = 3 KG/S**

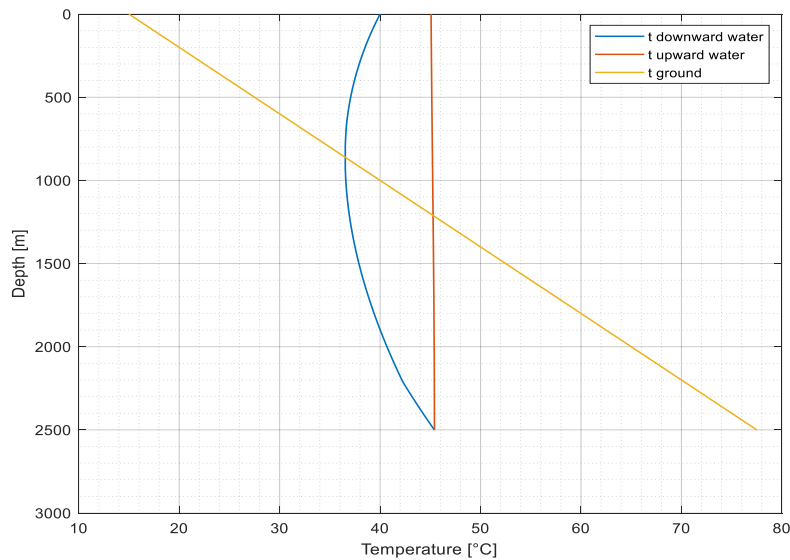


**FIGURE 24: CASE B-  $T_{INLET} = 40^{\circ}\text{C}$ ,  $T_{OUTLET} = 44.8^{\circ}\text{C}$ , FLOWRATE = 3 KG/S**



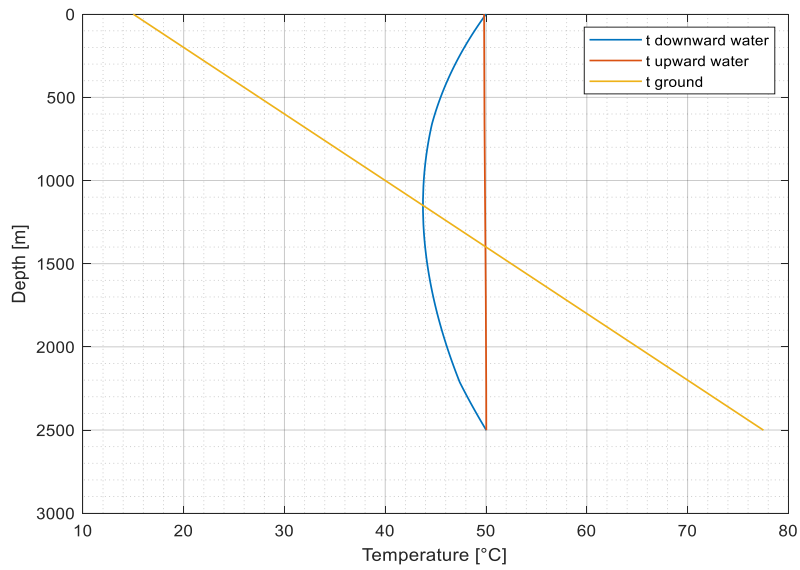


FIGURE 25: CASE C-  $T_{INLET} = 40^{\circ}C$ ,  $T_{OUTLET} = 44.8^{\circ}$ , FLOWRATE = 3 KG/S

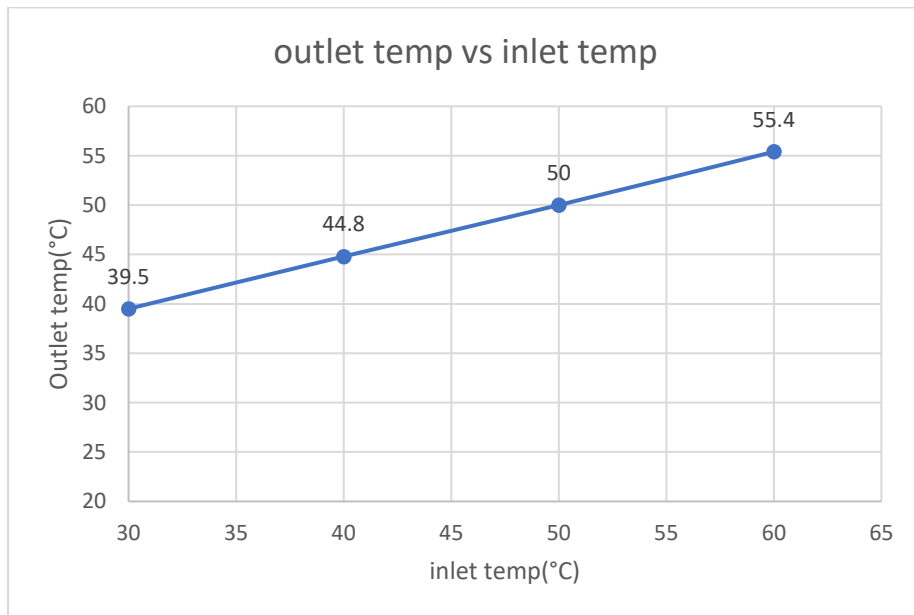


FIGURE 26: VARIATION IN OUTLET TEMP WITH CHANGE IN INLET TEMP

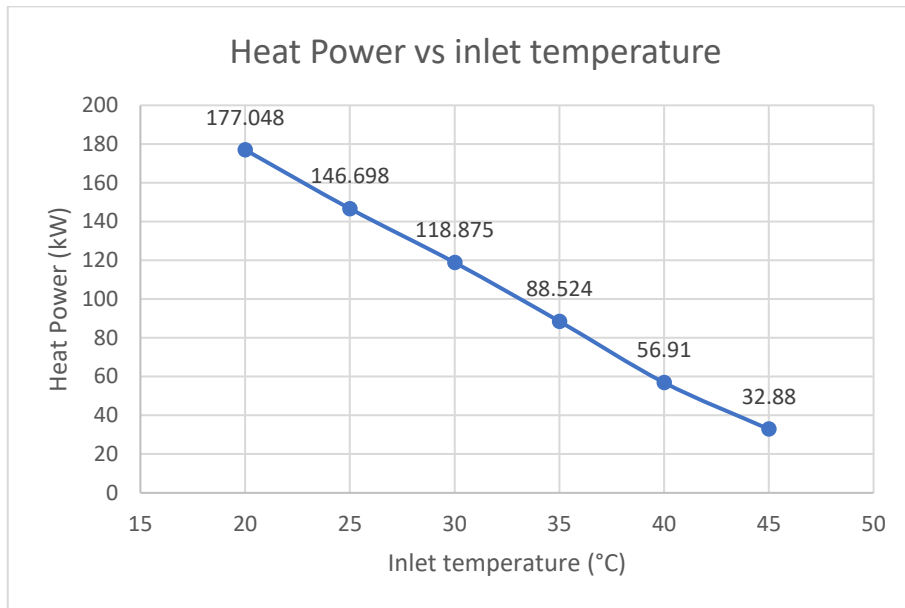


FIGURE 27: HEAT POWER VARIATION AS INLET TEMPERATURE CHANGES

According to Fig. 27, the heat power falls linearly as the inlet water temperature rises. The specific heat load is lowered by roughly 30 KW for every 5 degrees increase in inlet water temperature. This is a significant drop. This is mostly due to the fact that when the inlet fluid temperature rises, the temperature differential between the water and the earth underneath diminishes. As demonstrated in Fig. 26, as the inlet fluid temperature rises, the exit fluid temperature rises very little. The fluid temperature falls near the top of the outer pipe, suggesting that heat is transmitted from the water in the annular area to the earth below. And as the inlet fluid temperature rises, so does the heat loss. As a result, the topmost portion of the outer pipe should be thermally insulated.

To summarise, it is preferable to use a low inlet temperature to absorb more geothermal heat. If a high outlet temperature is necessary, the outer pipe should be insulated at least in the topmost section.

Impact of thermal conductivity of rock formations

The thermal conductivity of the rock formation is important in geological settings because of the heat transfer process between the rock and the fluid running within the outer pipe of the well that extracts heat from the rock. If the thermal conductivity of the rocks is higher, the heat transfer process can be accelerated by reducing the amount of time the rocks are in contact with the fluid. The following result depicts the effect of formation thermal conductivity on the working fluid's output temperature. The thermal conductivity of the rock, on the other hand, is fixed since it is determined by the kind of rock, saturation level, and position of the well. We have chosen two cases where minimum and maximum thermal conductivities are considered as reported in Table 6.

**TABLE 6: MINIMUM AND MAXIMUM VALUES OF THERMAL CONDUCTIVITY OF ROCKS (HAMDHAN & CLARKE [37])**

	CASE A (minimum)	CASE B (maximum)
Sands and Clays	2.45	3.8
Clays and Sandy marls	3.28	4.5
Marls, sands and gravels	2.77	3.9

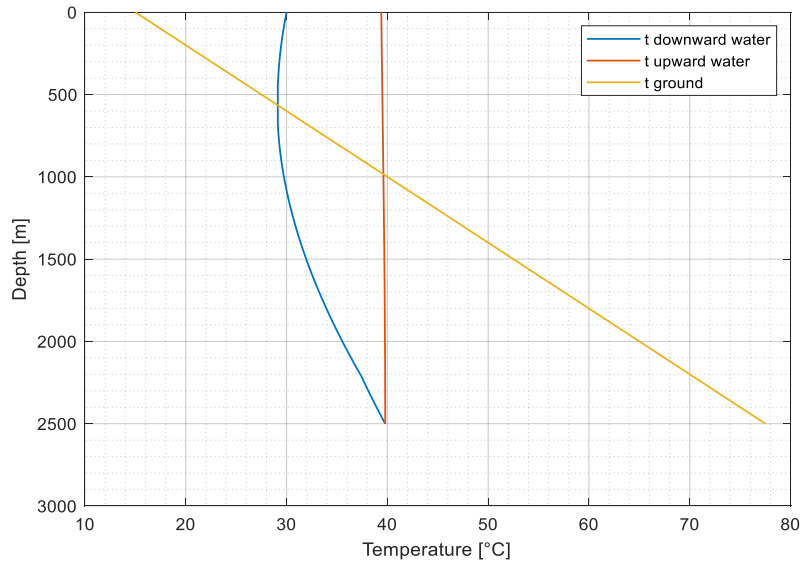


**FIGURE 28: CASE A- OUTLET TEMPERATURE = 39.5°C**

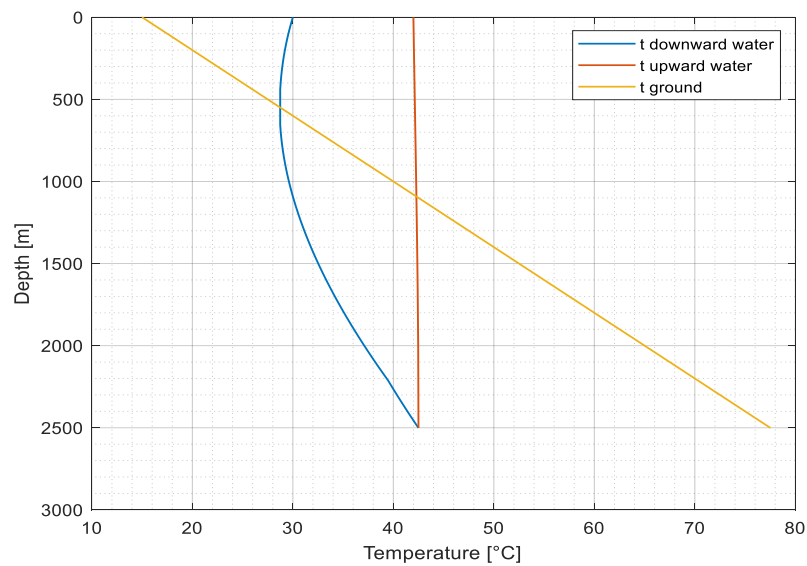


**FIGURE 29: CASE B- FIGURE 25 (B): OUTLET TEMPERATURE = 42°C**

Figures 28 & 29 indicate a 2.5-degree increase in output temperature when we evaluated the highest values of thermal conductivity in scenario B. This parameter is also affected by the depth of the well since the fluid will be in contact for a longer period of time as the depth grows and can extract a greater quantity of heat than in shallower wells.

Influence of outer diameter:

Consider the two options of altering the outer diameter while maintaining the inner diameter and thickness of the inner pipe constants, as illustrated in cases A and B (Table 7), with an input temperature of 30°C and a flowrate of 3 kg/s.

**TABLE 7: GEOMETRICAL PARAMETERS FOR CASTEGGIO**

Tube sizing	CASE A [28]	CASE B
ID (mm)	77	77
ID <sub>insulation</sub> (mm)	139.2	139.2
OD (mm)	150	200

Fig. 30 & 31 demonstrate that expanding the outer diameter from 150 to 200 mm results in a very minor change in outlet temperature of 0.5°C and a rise in thermal power from 120.14 to 126.463 kW. Because the fluid velocity reduces as the outer diameter rises, the entrance velocity in the annular space decreases at an invariant inlet flowrate, allowing enough time for heat exchange between the water in the annular space and the soil underneath.

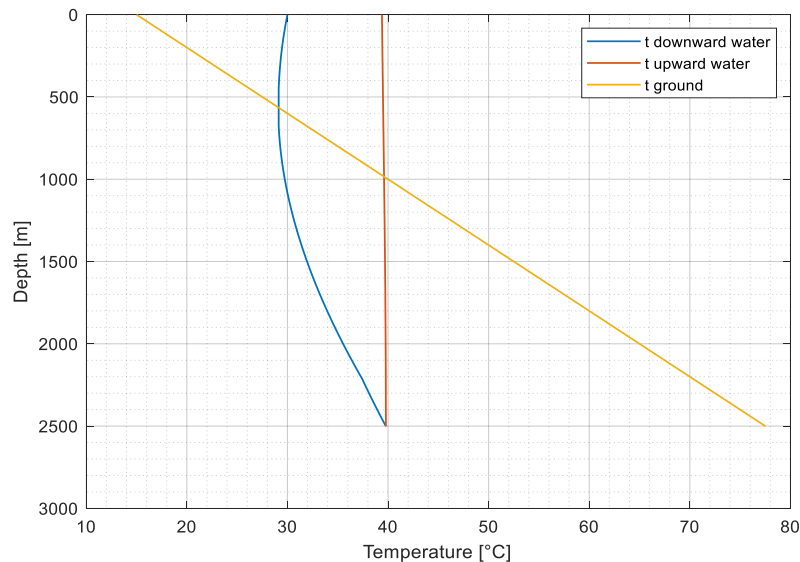


**FIGURE 30: CASE A- OUTLET TEMP = 39.5°C, Q = 120.14 kW**

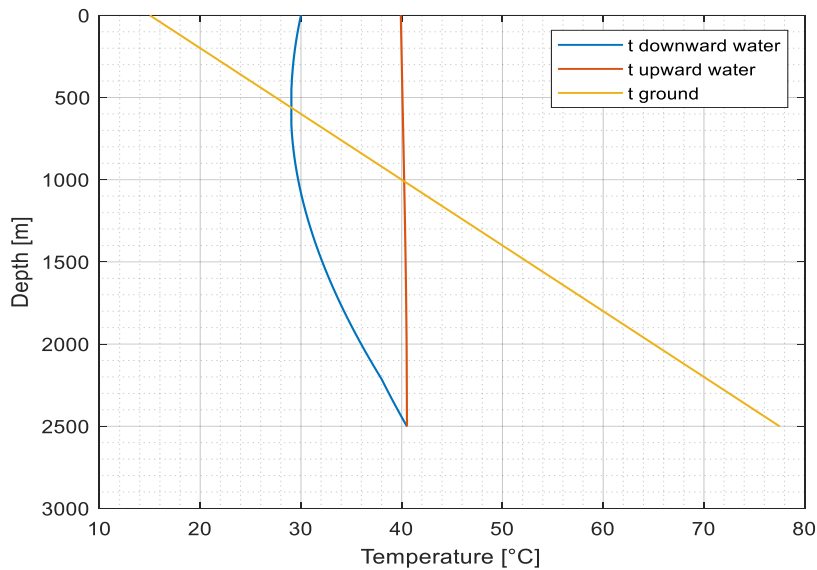


FIGURE 31: CASE B- OUTLET TEMP = 40°C, Q = 126.46 kW

As the outer diameter increases, the intake fluid velocity drops, and therefore the pumping power required lowers. The pumping power gradually diminishes as the outer diameter increases. In brief, as the outer pipe diameters grow, the thermal power required increases but the pumping power required reduces. It is beneficial for energy savings, but as the diameter of the outer pipe grows, so does the expense of installing the underground pipe system. As a result, in practice, both the heat exchanger's thermal performance and economic aspects should be considered when determining the outer pipe diameter.

#### Thermal conductivity of the inner pipe

The working fluid flows upward via the inner pipe after absorbing heat from the surrounding rocks. During this time, the heated fluid exchanges heat with the cold fluid in the annular gap via conduction and convection, a process known as thermal short-circuiting. The high-temperature differential causes heat loss between the heat carrier in the outer and inner pipe. Thermal insulation is applied to the inner pipe to reduce heat losses, or a low thermal conductivity inner pipe material is utilized to decrease heat losses between the fluids. The following findings demonstrate the effect of the insulator on the working fluid's output temperature.

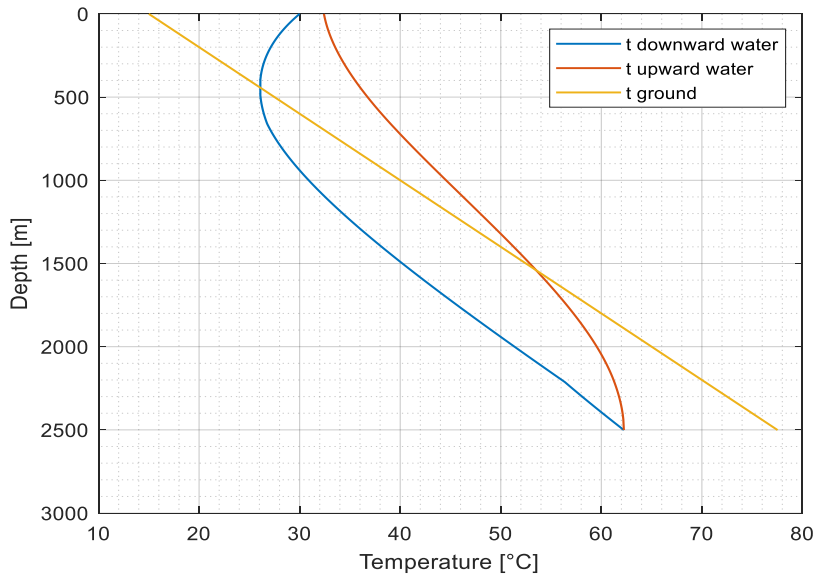


FIGURE 32: CASE A- TOUT = 32.2°C @  $\lambda = 0.25^\circ\text{C}$ , TINLET = 30°C, FLOWRATE = 0.5 KG/S

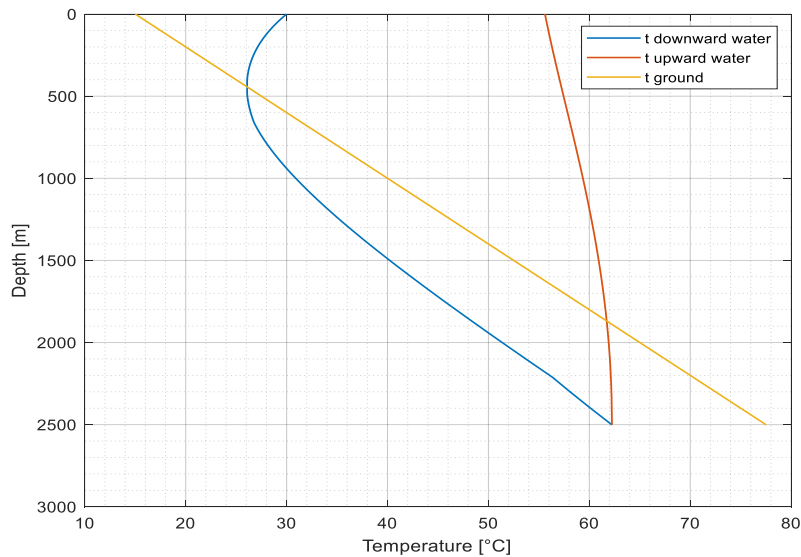


FIGURE 33: CASE B- TOUT = 55.8°C @  $\lambda = 0.025 \text{ W/M.K}$ , FLOWRATE = 0.5 KG/S, TINL = 30°C

When the results of both cases (Fig 32 & 33) are compared, the output temperature varies drastically about 23.6°C. If the depth of the well is higher, the influence of the insulation on thermal heat extraction will be greater. As a result, using thermal insulation is a key element for preventing heat losses and increasing efficiency.

Changing the injecting fluid flowrate from 0.5 kg/s to 3 kg/s yields very different outcomes. Looking at Fig. 34 & 35 simulated at 3 kg/s flowrate, the outlet temperature in both cases differs from 3.4°C. This is due to the greater flowrate value; as the inlet flowrate grows, the fluid's velocity increases and the contact time between the fluid and the underground formations decreases; as a consequence, it extracts less heat. The heat exchange period between the heat carriers of the inner pipe and the outer pipe will be shorter

as the flowrate increases in the inner pipe. Therefore, the heat losses will be reduced and the thermal conductivity of the insulator on the inner pipe will have a lower impact as it had in Fig. 32 & 33.

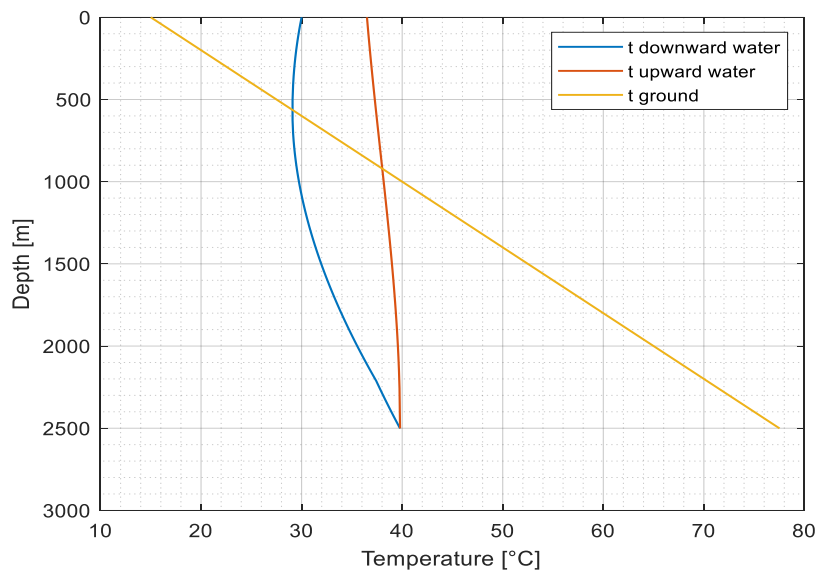


FIGURE 34: CASE A - TOUT = 36.4°C @ FLOWRATE = 3 KG/S & THERMAL CONDUCTIVITY = 0.25 W/M.K

The heat loss transmitted from the fluid in the inner pipe to the fluid in the outer pipe increases as the heat conductivity of the inner pipe increases. And as the water flows higher in the inner pipe, the temperature differential between the water in the inner and outside pipes grows, increasing heat loss and lowering the output fluid temperature. Furthermore, when the fluid temperature in the circular space rises, the temperature differential between the water in the annular space and the earth underneath decreases. As a result, the heat load from the earth will be reduced. In summary, the material of inner pipe with high heat conductivity would result in large heat loss under the effect of thermal short-circuiting.

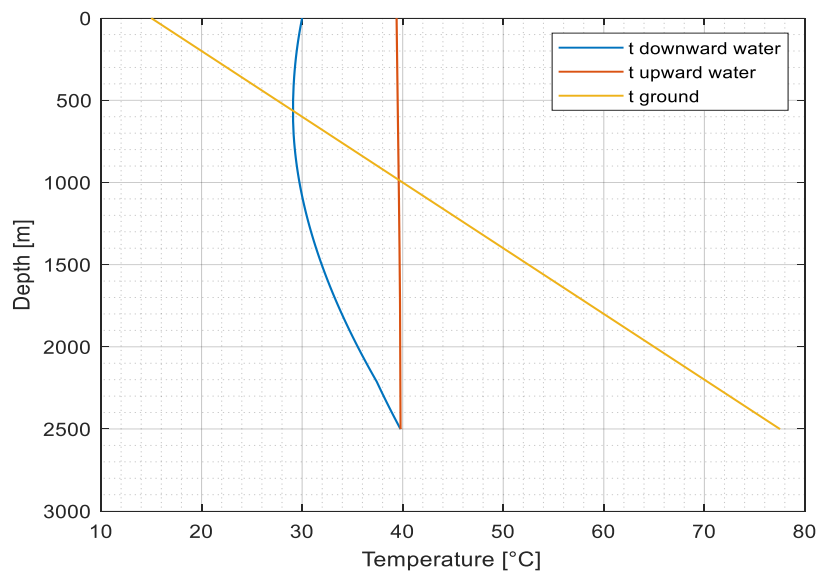


FIGURE 35: CASE B - TOUT = 39.5°C @ FLOWRATE = 3 KG/S & THERMAL CONDUCTIVITY = 0.025 W/M.K

Thickness of the thermally insulated inner pipe:

Further investigation has been carried out on thermal insulation of inner pipe by considering the flowrate of 0.5 kg/s,  $T_{inlet} = 30^{\circ}C$ , thermal conductivity of insulator = 0.025 W/m.K, outer pipe diameter = 150 mm and inner pipe diameter = 77 mm as reported in Table 8 & 9.

**TABLE 8: DIAMETER AND THICKNESS OF THERMALLY INSULATED CENTRE PIPE**

	CASE A	CASE B	CASE C
Flowrate (kg/s)	0.5	0.5	0.5
Diameter of inner pipe (mm)	77	77	77
Thickness (mm)	62.2	30	20
Diameter (insulation) (mm)	139.2	107	97
Outlet temp ( $^{\circ}C$ )	55.8	51.4	47.9

The outcome after putting the above-considered values in the MATLAB code shows the reduction in outlet temperature as the thickness of the insulation increases.

**TABLE 9: DIAMETER & THICKNESS OF THERMALLY INSULATED CENTRE PIPE**

	CASE A	CASE B	CASE C
Flowrate (kg/s)	3	3	3
Diameter of inner pipe (mm)	77	77	77
Thickness (mm)	62.2	30	20
Diameter (insulation) (mm)	139.2	107	97
Outlet temp ( $^{\circ}C$ )	39.5	39	38.6

Here in Table 9, the flowrate rate is taken 3 kg/s, due to the large value of mass flowrate, the variation in outlet temperature is very small. A large flowrate gives high thermal power but reduces the outlet temperature while reducing the need of thermally insulated pipe.



## TURBIGO 1

### Impact of inlet flow rate

When comparing the findings in figure 36,37,38 & 39, it can be concluded that using a flowrate of 0.5–1 kg/s gives a greater value of outlet temperature than using a flowrate of 3 kg/s, which results in a lower value of fluid outlet temperature. When the flowrate is higher, the fluid is in touch with the rock formation for a shorter period of time while moving downward, and it is unable to extract enough heat from the formations. When the flow rate is larger, however, the returning fluid loses less amount of heat.

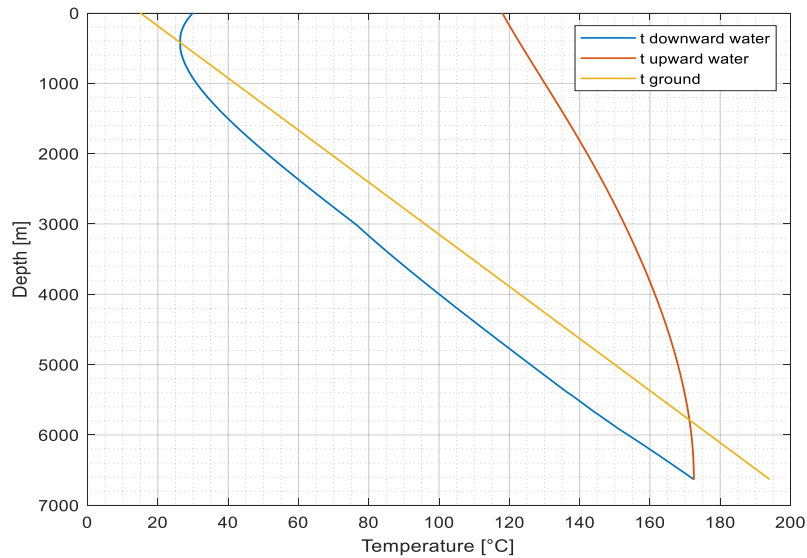


FIGURE 36: CASE A -  $T_{INLET} = 30^{\circ}\text{C}$ , FLOWRATE = 0.5 KG/S,  $T_{OUTLET} = 120^{\circ}\text{C}$

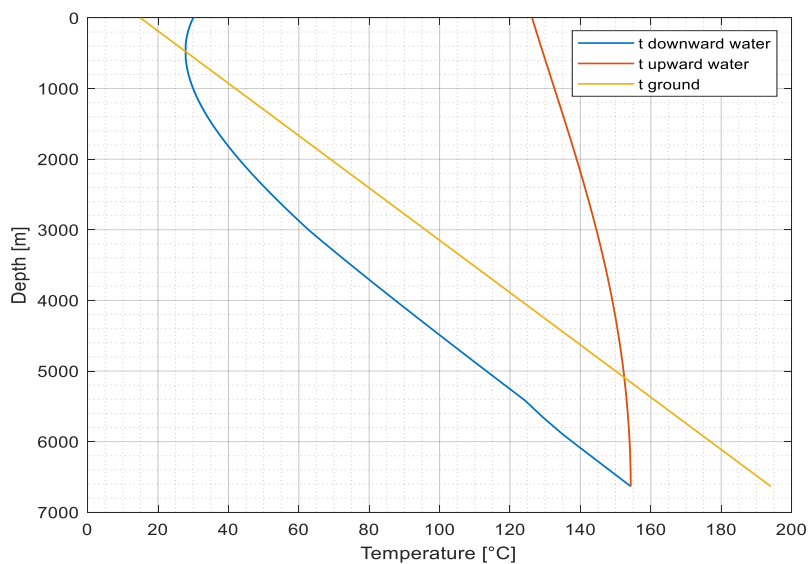


FIGURE 37: CASE B -  $T_{INLET} = 30^{\circ}\text{C}$ , FLOWRATE = 1 KG/S,  $T_{OUTLET} = 126^{\circ}\text{C}$

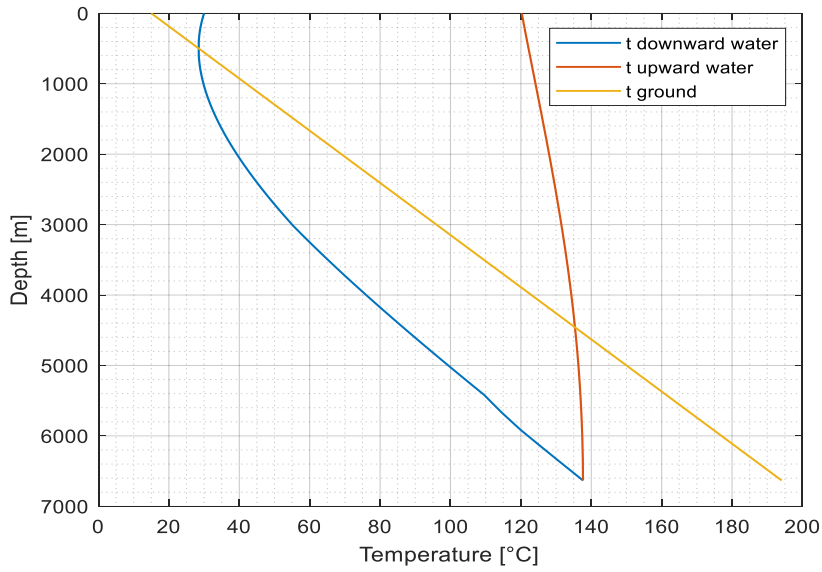


FIGURE 38: CASE C - TINLET = 30°C, FLOWRATE = 1.5 KG/S, TOUTLET = 120°C

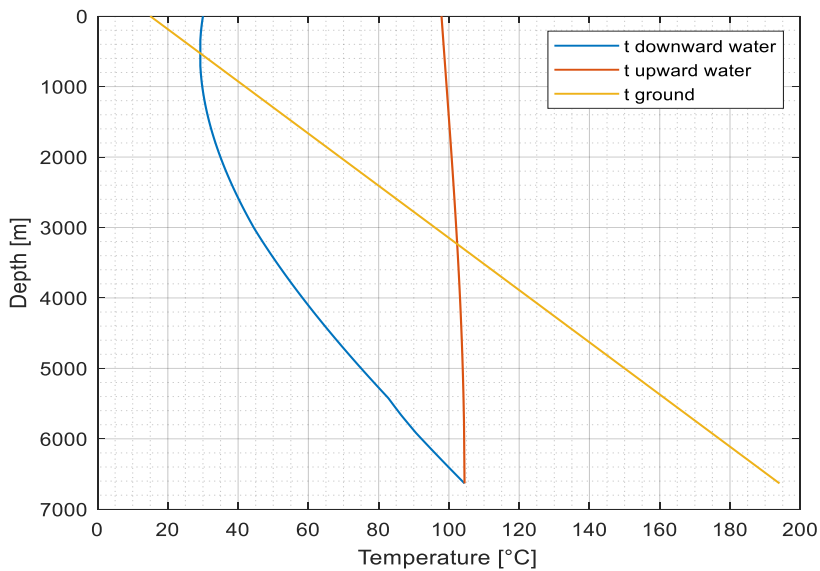


FIGURE 39: CASE D - TINLET = 30°C, FLOWRATE = 3 KG/S, TOUTLET = 98°C

Figure 40 illustrates that, at initially, the well's output temperature rises as the flowrate rises. However, there is a limit beyond which the outlet temperature rises. If we raise the flowrate beyond that point, the output temperature will drop. Furthermore, increasing the flowrate necessitates the use of more pumping power, which raises the overall cost of the system.

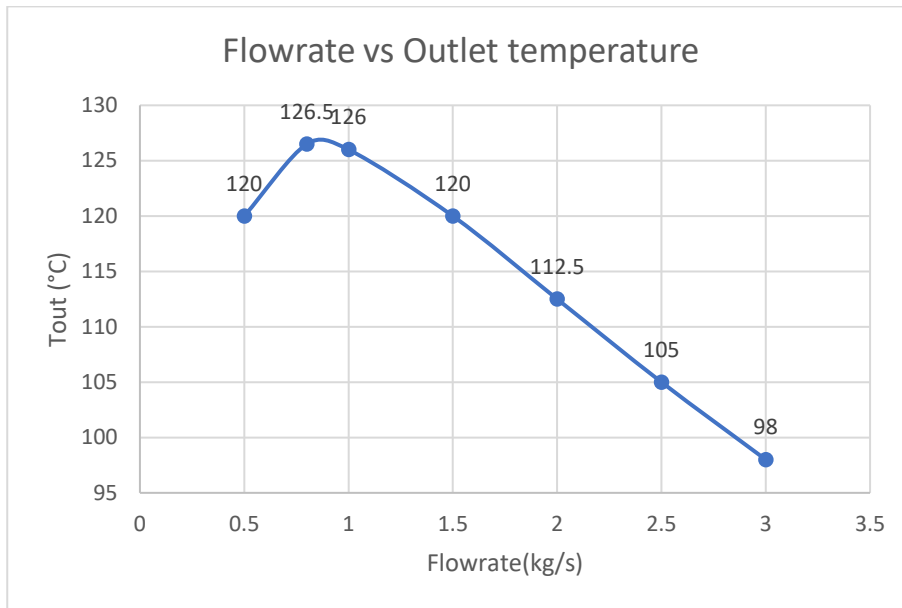


FIGURE 40: VARIATION IN OUTLET TEMP AS FLOWRATE CHANGES

Figure 40 shows that, the output temperature of the well increases linearly from 98 °C to 126.5°C, as the flowrate of the injecting fluid decreases from 3 kg/s to 0.8 kg/s.

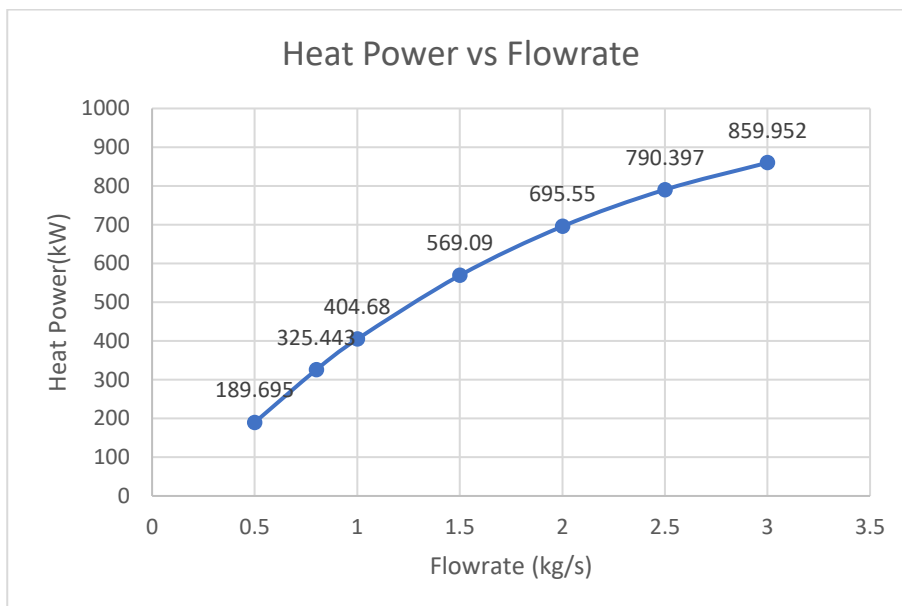


FIGURE 41: HEAT POWER VS FLOWRATE

Figure 41 depicts the relationship between heat power and flowrate; as the flowrate increases, so does the thermal power. When the flowrate is increased from 0.5 to 3 kg/s, the thermal power rises from 189.695 kW to 859.952 kW.

### Impact of inlet temperature

Figure 42 shows an inlet temperature of 30°C and a flowrate of 3 kg/s. The temperature at the outflow is about 98°C. As the fluid inlet temperature rises to 80°C while the flowrate remains constant, the outlet temperature rises to 110.9°C (Figure 43). If we look at the blue curve in fig 42, we can see that there is a reverse heat transfer process from the surface to 1000 meters depth. Because the temperature of the formation down to 1000 m deep is lower than the temperature of the fluid, heat is transferred from the fluid to the rocks because heat always goes from high to low temperature. There, the temperature of the fluid first decreases till the depth of 1000 m, then starts gaining heat from the hot rocks.

By increasing the input temperature from 30 to 80 degrees, there will be a significant temperature differential between the rocks and the fluid up to a depth of about 2000 meters since the surface is cold when injected fluid, resulting in reverse heat transfer. As seen in figure 43, the temperature of the fluid decreases until it reaches a depth of 1800 m, at which point it begins to rise.

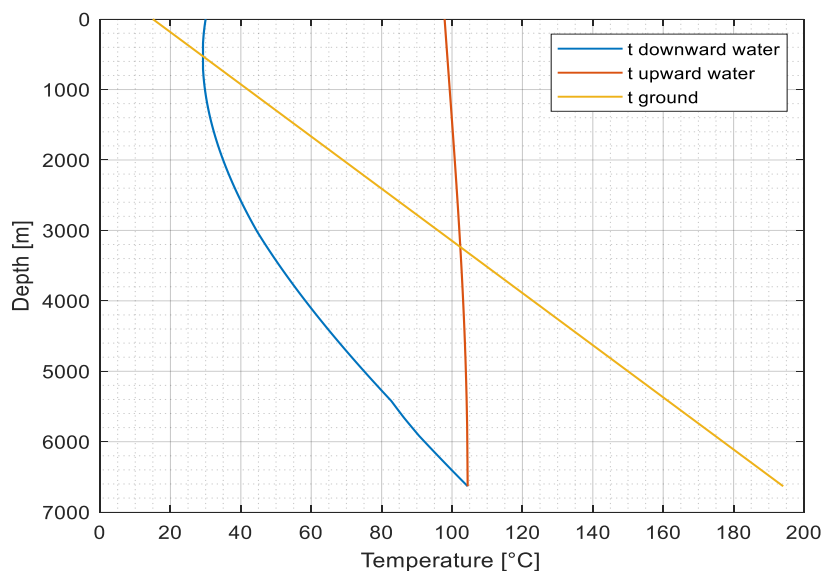


FIGURE 42: CASE A - TINLET = 30°C, FLOWRATE = 3 KG/S. TOUTLET = 98 °C

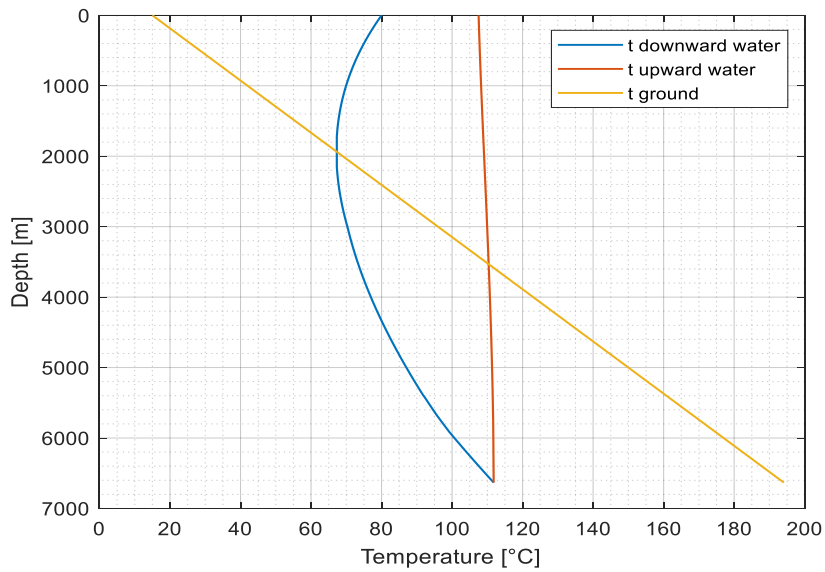


FIGURE 43: CASE B -  $T_{INLET} = 80^{\circ}\text{C}$ ,  $\text{FLOWRATE} = 3 \text{ KG/S}$ .  $T_{OUTLET} = 110.9^{\circ}\text{C}$

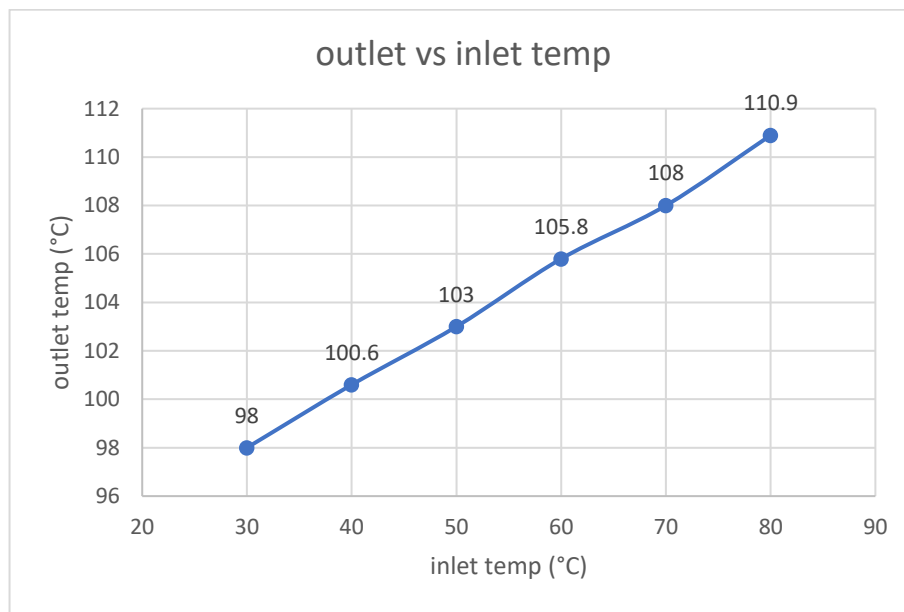


FIGURE 44: VARIATION IN OUTLET TEMP AS INLET TEMPERATURE CHANGES

As a result, increasing the intake temperature by  $50^{\circ}\text{C}$  raises the output temperature by  $12.9^{\circ}\text{C}$ . Heat transmission reduces approximately linearly as the input temperature rises. Furthermore, when the soil temperature at the top of the casing is lower than the fluid temperature in the casing, heat from the water in the pipe penetrates the soil beneath, and the loss increases as the inflow water temperature rises. As a consequence, choosing a lower intake temperature will allow you to harvest more geothermal energy.

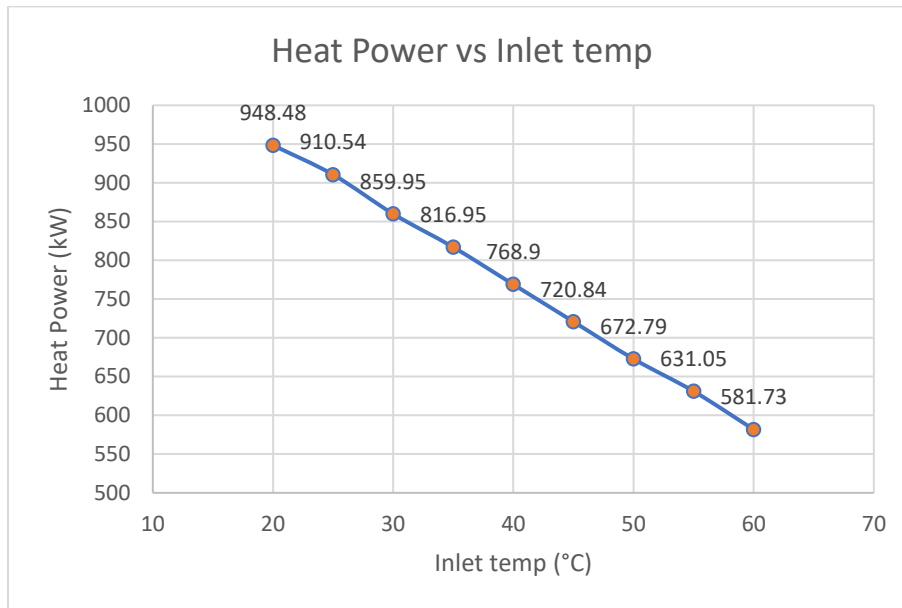


FIGURE 45: HEAT POWER CHANGES ALMOST LINEARLY WITH INLET TEMPERATURE

According to Fig. 45, the heat power falls practically linearly as the intake water temperature rises. The specific heat load is lowered by 45 KW for every 5 degrees increase in intake water temperature. This is a significant drop. This is mostly due to the fact that when the intake fluid temperature rises, the temperature differential between the water and the earth underneath diminishes. As illustrated in Fig. 44, as the inlet fluid temperature rises, the exit fluid temperature rises only little. The fluid temperature falls near the top of the outer pipe, suggesting that heat is transmitted from the water in the annular area to the earth below. And as the intake fluid temperature rises, so does the heat loss. As a result, thermal insulation measures should be implemented in the outer pipe's topping portion.

Impact of thermal conductivity of underground formations

Thermal conductivity can be measured in the laboratory or in situ, such as in a borehole or deep well, by activating a heating element and monitoring the temperature rise over time. It is determined by several factors, including (1) the chemical composition of the rock (i.e., mineral content), (2) fluid content (type and degree of saturation of the pore space; the presence of water increases thermal conductivity (i.e., improves heat flow), (3) pressure (a high pressure increases thermal conductivity by closing cracks that inhibit heat flow), (4) temperature, and (5) isotropy and anisotropy.

Here in Table 10, we considered the minimum and maximum possible values of thermal conductivities from literature [37-44].

**TABLE 10: MINIMUM AND MAXIMUM THERMAL CONDUCTIVITIES OF UNDERGROUND FORMATIONS**

Lithology	CASE A (min values of k) (W/m.K)	CASE B (max values of k) (W/m.K)
Sands, pebbles and clays	2.45	3.2
Clays, sand and pebbles	2.45	3.2
Sand and clays	2.45	3.2
Clay, sandstones, conglomerates	2.74	3.68
Marls and limestone	2.72	4.5
Marls, sandstone and limestones	2.15	3.5
Marls, limestone, dolomite and selce	2.24	4.2
Limestone, dolomite, marls, clays and sand	2.5	3.9

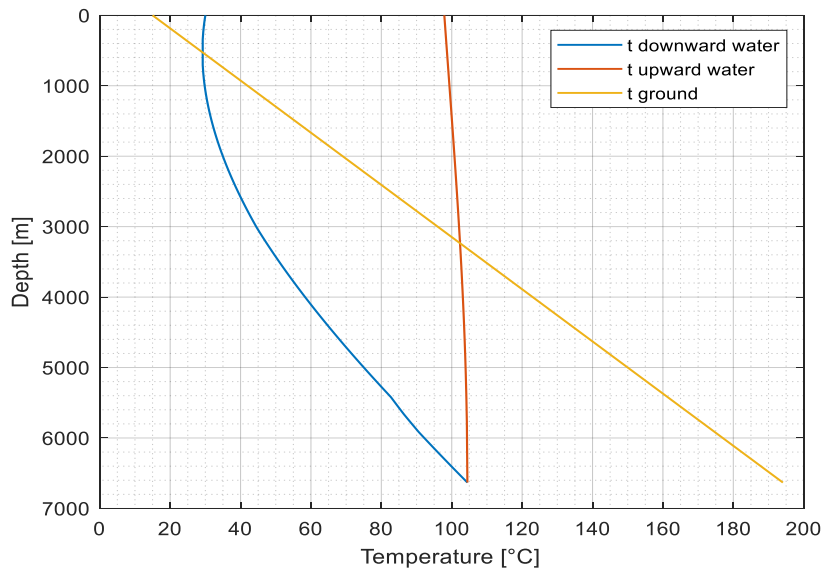


**FIGURE 46: CASE A - TINLET = 30°C, FLOWRATE = 3 KG/S, TOUTLET = 98°C**

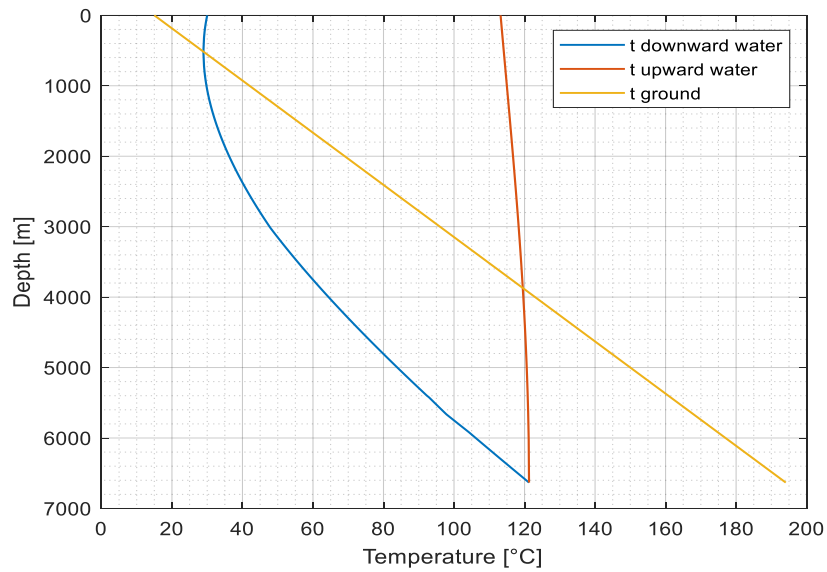


FIGURE 47: CASE B - TINLET = 30°C, FLOWRATE = 3 KG/S, TOUTLET = 113.6°C

As illustrated in Figure 46 & 47, increasing the thermal conductivity of the underground formation raises the output temperature by 15.6°C, increasing the thermal power to 1057.234 kW or 1 MW. Because the data is derived from the literature, it may differ depending on the location of the wells. In order to obtain the correct results, more practical research on the thermal conductivity values of rock formations must be conducted.

Diameter of the outer pipe

Considering the two possibilities of changing the outer diameter while maintaining the inner diameter and thickness of the inner pipe constants, with an inlet temperature of 30°C and a flowrate of 3 kg/s as shown in cases A and B reported in Table 11, as we did for CASTEGGIO, just to analyze the impact of outer diameter on the heat exchange mechanism.

**TABLE 11: GEOMETRICAL PARAMETERS OF TURBIGO**

Tube sizing	CASE A (Alimonti)	CASE B
ID (mm)	77	77
ID <sub>insulation</sub> (mm)	139.2	139.2
OD (mm)	150	200
Outlet temp (°C)	98	100



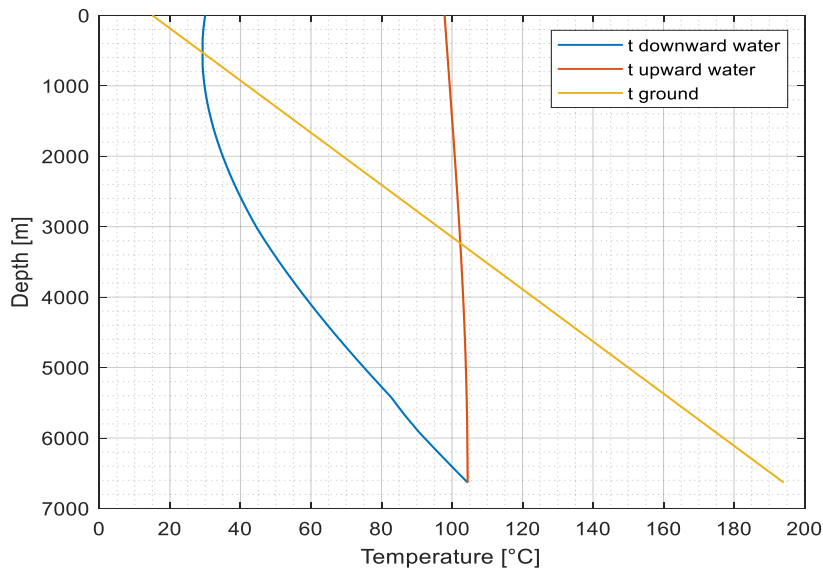


FIGURE 48: CASE A - TINLET = 30°C, FLOWRATE = 3 kg/s, TOUTLET = 98°C

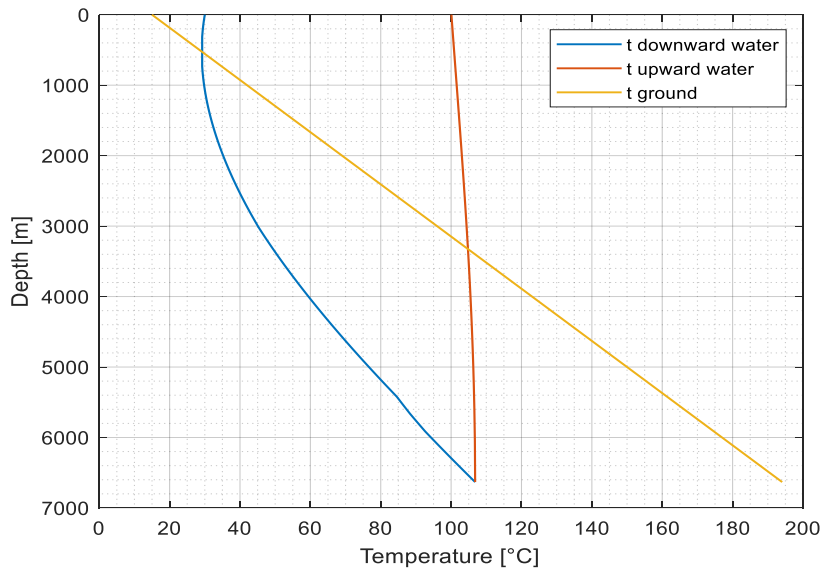


FIGURE 49: CASE B - TINLET = 30°C, FLOWRATE = 3 kg/s, TOUTLET = 100°C

Fig. 48 & 49 indicate that by expanding the outer diameter from 150 to 200 mm, the output temperature rises by 2°C and the thermal power climbs from 859.89 kW to 885.244 kW. The input velocity in the annular space slows as the outer diameter rises at an invariant inlet flowrate, allowing enough time for heat exchange between the water in the annular space and the soil underneath. It is worth noting that altering the outer diameter, inner diameter, and thickness of the inner pipe's thermal insulation all at the same time can create a significant impact in heat exchange performance.

Thermal conductivity of the inner pipe

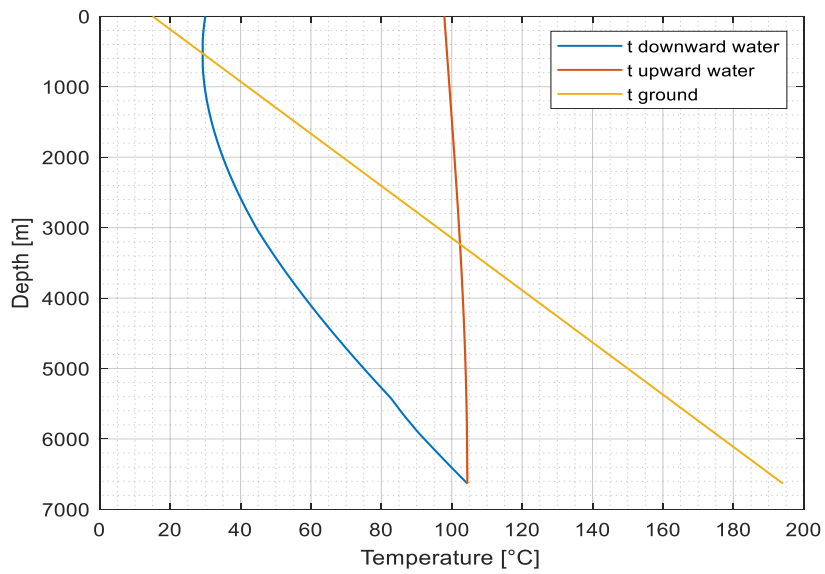


FIGURE 50: CASE A - THERMAL CONDUCTIVITY = 0.025 W/M.K, TOUTLET = 98°C

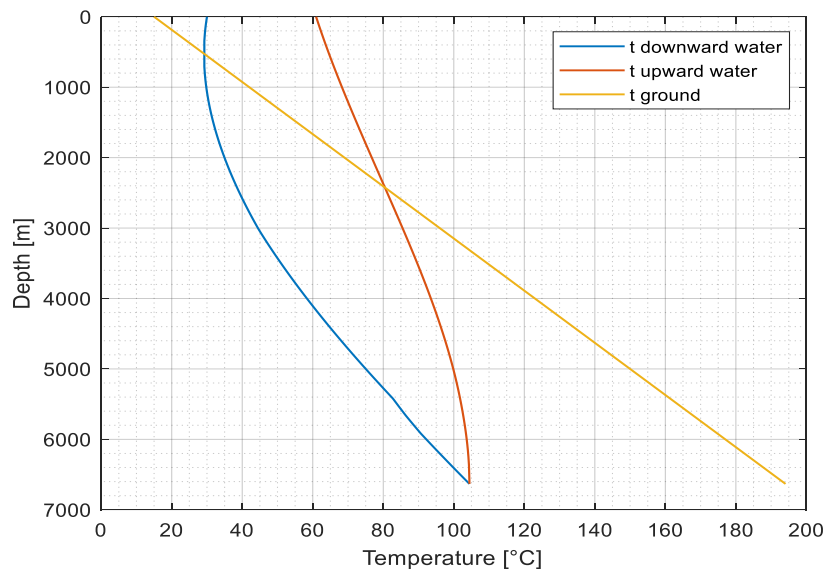


FIGURE 51: CASE B - THERMAL CONDUCTIVITY = 0.25 W/M.K, TOUTLET = 61°C

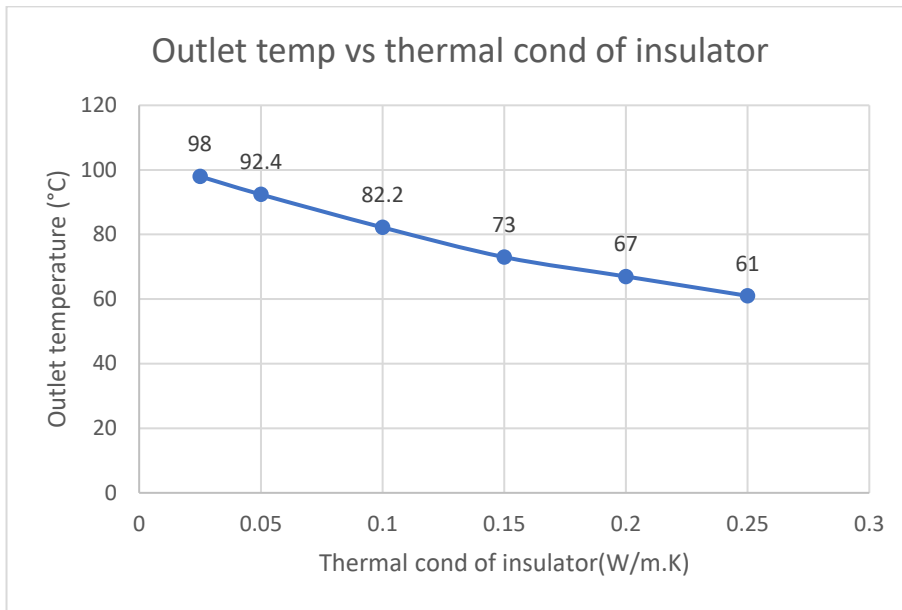


FIGURE 52: OUTLET TEMPERATURE VARIATION WITH THERMAL CONDUCTIVITY OF INSULATED CENTRE PIPE

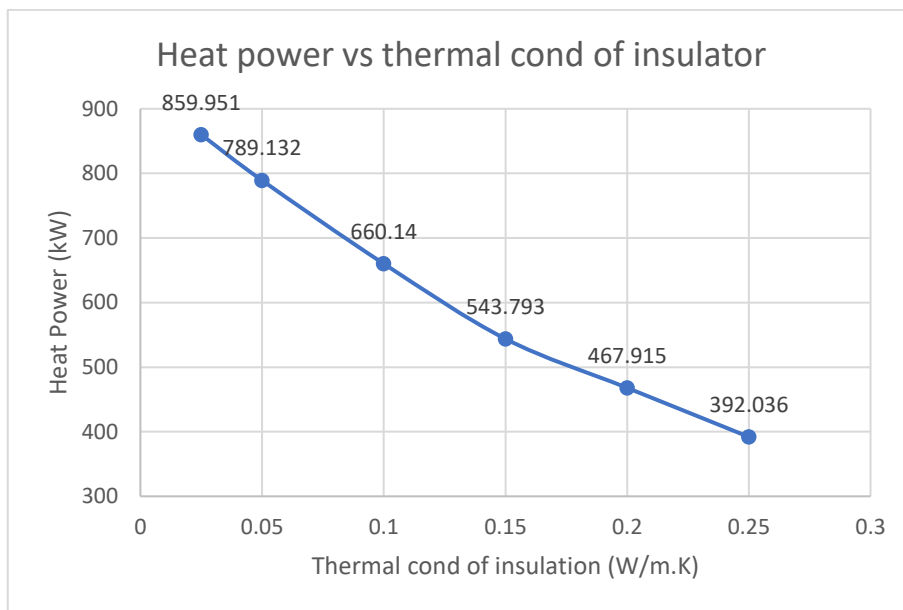


FIGURE 53: HEAT POWER TREND VS THERMAL CONDUCTIVITY OF INNER PIPE

When comparing the results of Figures 50 & 51, the difference in the output temperature is about 37 degrees when the thermal conductivity is changed from 0.25 to 0.025 W/m.K. The temperature at the bottomhole is roughly equal in both cases, but if we look closely at the red line in the graph that shows the trend of the working fluid going upward, we can see that there are more heat losses in case B where thermal conductivity is quite high, as it exchanges heat with the wall and the cold fluid in the annular region. Overall, the thermal conductivity of the insulating material is a critical characteristic that must be as low as possible in order to decrease heat losses in the borehole's inner pipe. In conclusion, the high heat conductivity of the inner pipe material would result in significant heat loss as a result of thermal short-

circuiting. As the outlet temperature increases (Figure 52), difference in inlet and outlet fluid temperature increases. Thus, the heat power increases with the reduction in thermal conductivity values as shown in Figure 53.

Thickness of the thermally insulated inner pipe:

**TABLE 12: DIAMETER AND THICKNESS OF THERMALLY INSULATED CENTRE PIPE**

	CASE A	CASE B	CASE C
Flowrate (kg/s)	3	3	3
Diameter of inner pipe (mm)	77	77	77
Thickness (mm)	62.2	30	20
Diameter (insulation) (mm)	139.2	107	97
Outlet temp (°C)	98	93	89
Heat Power (kW)	859.95	796.72	746.134

The decrease in outlet temperature and heat power, as shown in Table 12, justified that increasing the thickness of insulation can be advantageous in improving the thermal performance of the well.

#### 4. COMPARISON BETWEEN THE WELLS

Two exploratory wells, CASTEGGIO and TURBIGO, were chosen as case studies in our thesis study to assess the influence of physio-chemical and technical characteristics of rocks and the wellbore, respectively.

CASTEGGIO is 2501 meters deep, with a geothermal gradient of 25 degrees Celsius every kilometer. In this scenario, the temperature at the bottom of the well is about 70°C. The working fluid is water, which is injected into the annular area and returns to the surface via the inner pipe after extracting heat from the formations. The depth of TURBIGO is approximately 6632.7 m, and the geothermal gradient is 27°C/km. The temperature at the well's bottomhole is about 184°C. In MATLAB, an existing approach is used to assess the influence of physio-chemical and technical factors by altering their values from the literature.

When these two wells are compared, the outlet temperature and thermal power that can be reached in the case of CASTEGGIO while retaining the flowrate and inlet temperature at 3 kg/s and 30°C are 39.5°C and 120.412 kW, respectively. However, for TURBIGO, the exit temperature and heat power of the fluid at the surface are 98°C and 859.952 kW, respectively, when the flowrate and inlet temperature are the same as in CASTEGGIO. Other characteristics such as thermal conductivity of rocks, inlet fluid temperature, outer diameter, and thermal conductivity of inner pipe insulation can be used to further vary the output temperature and thermal power.

The large variations in output temperature and heat power are mostly attributable to the two wells' differing depths and geothermal gradients. The depth of the wellbore is a very important element in drawing heat from the earth; as we go deeper, the temperature of the rocks rises based on the geothermal gradient. We might claim that heat extraction is affected by the depth of the BHE. However, raising the depth of the well eventually raises the cost of drilling, pipe installation, grouting materials, and so on. As a result, the optimum design varies depending on the depth of the well.

According to the Lindal diagram (Figure 7), electricity generation from CASTEGGIO is not viable since the highest outlet temperature we are obtaining from this well is not in the range (75 – 145) °C of electricity production, i.e., by using the Organic Rankine Cycle or Kalina Cycle. In the case of TURBIGO, however, the maximum output temperature falls within the range of power production. So, we can claim that energy generation is conceivable with TURBIGO, but further economic research is required before installing a geothermal power plant or converting it into a geothermal well.

To summarize, CASTEGGIO is not appropriate for power generation, but it may be used to generate heat for direct purposes such as fish breeding, balneology, de-icing, floor heating swimming pools, mushroom culture, decomposition, biomass, and animal breeding.

It is possible to produce electricity from well TURBIGO, as well as direct usage such as intense defrosting, sugar refining, lightweight concrete structure drying, vegetable drying, house heating, greenhouse heating, and drinking water generation in the distillation process.

The above-mentioned applications are reliant not only on the outlet temperature and thermal power, but also on the positioning of the wells in the proper area where geothermal energy may be used safely, cheaply, and efficiently. Heat, unlike oil and gas, is difficult to transfer over long distances because it necessitates the installation of costly insulated flowlines. If employed as part of a direct use heating opportunity, a distance of 10 kilometres or less from well to boiler is required for present economics [45].

## 5. CONCLUSIONS

The study used available information on exploratory hydrocarbon wells to apply a simplified co-axial borehole heat exchanger model to two wells located in northern Italy (Casteggio 2 Well and Turbigio 1 Well). We performed a number of sensitivity analysis to point out the effect of rock formation properties (thermal conductivity, heat capacity and density) and the technical parameters associated with the working fluid and the wellbore on the heat transfer performance of the Wellbore heat exchanger. The main aim of this work is to identify the parameters that could be varied to enhance the heat transfer process and to make the system more efficient on the subject of thermal power and outlet temperature of the circulating fluid.

In our developed thesis work, an existing model implemented in MATLAB software was used to examine the impact of some characteristic parameters of rocks like thermal conductivity, specific heat and density on the extracted amount of heat. Also, a sensitivity analysis was carried out by varying the flowrate of the working fluid, inlet fluid temperature, the outer diameter of the pipe, thermal conductivity of insulating material and the thickness of insulation. The results show a significant difference in the potential amount of thermal heat and the outlet temperature between analyzed wells. In accordance with these investigations, we have drawn the following conclusions.

- (1) As the inlet flow rate increasing from 0.5 to 3 kg/s, the outlet temperature decreases from 55.8 to 39.5 °C, and the heat power increases from 54.38 to 120.142 kW for CASTEGGIO. In the case of TURBIGIO, the outlet temperature decreases from 120 to 98°C and the thermal power rises from 189.695 to 589.95 kW. The pump power increases as the flowrate rises. So, the economic and reasonable inlet flow rate should be chosen according to the energy consumption of the pump.
- (2) As the inlet fluid temperature increasing from 30 to 40 °C, the outlet temperature rises from 39.5 to 44.8°C, however, the heat power decreases from 118.875 to 56.91 kW in case of CASTEGGIO. For TURBIGIO heat power reduces from 859.95 to 581.73 kW and outlet temperature rises from 98 to 105.8 °C as the inlet fluid temperature increases from 30 to 60°C. Furthermore, when the subsurface temperature at the top of the casing is lower than that of the fluid in the casing, heat enters the underground formations from the water in the pipe, and the loss increases as the inlet water temperature increases. As a result, the lower inlet temperature should be selected to extract more geothermal energy.
- (3) Thermal conductivity of the rocks plays a key role for wells having greater depth like TURBIGIO. The analysis was done by choosing two sets of thermal conductivity values as the minimum and maximum values depending upon the saturation level of the formations. The outlet temperature reaches from 39.5 to 42°C in the case of CASTEGGIO and rises from 98 to 113.6°C for TURBIGIO as we put the maximum thermal conductivity values instead of minimum in our analysis. Also, the heat power for TURBIGIO rises from 859.95 kW to 1 MW.
- (4) The heat power and the outlet temperature increase with the increasing of outer pipe in both the wells but it has a very small effect on both the parameters as we discussed in the results. For CASTEGGIO, the outlet temperature rises from 39.5 to 40°C and the

heat power increases from 120.14 to 126.46 kW. However, in the case of TURBIGO, the rise in outlet temperature and heat power are of 2 °C and 25.354 kW respectively due to the larger depth. It is advantageous to energy conservation, but as the diameter of the outer pipe grows, so does the expense of installing the underground pipe system. As a result, in practice, both the heat exchanger's thermal performance and economic aspects should be considered when determining the outer pipe diameter.

- (5) Under the impact of thermal short-circuiting, the material of the inner pipe with high heat conductivity would result in significant heat loss. For CASTEGGIO, as the thermal conductivity increasing from 0.25 to 0.025 W/m.K considering the flowrate of 3 kg/s & inlet fluid temperature of 30°C, the rise in outlet temperature is 3.1°C. However, in case of TURBIGO, for the same flowrate and inlet fluid temperature, the rise in outlet temperature and heat power are 37°C and 467.92 kW, respectively. Much better thermal performance can be obtained by using the material of low thermal conductivity. Here, the depth and geothermal gradient of the well are very crucial and making a huge difference in the performance of the wells.
- (6) The thickness of the inner pipe insulation can be of great significance if properly analyzed with the outer pipe diameter and the inlet flowrate simultaneously to achieve the maximum output in terms of thermal energy. The thickness of insulation has a great influence on the performance of heat power for TURBIGO. However, it shows a very small effect for CASTEGGIO due to the variation in depth and the bottomhole temperature. The result shows the reduction in thermal power from 859.95 to 746.134 kW as the thickness reduces from 69.2 to 20 cm for TURBIGO. Nevertheless, the influence on CASTEGGIO is very small, as the outlet temperature decreases from 39.5 to 38.6°C only and the thermal power reduces from 120.14 to 108.76 kW.

Furthermore, in order to get the best design, all of the factors we covered in our research must be assigned at the same time. Future investigation is needed to improve the precision of the suggested study; the primary assumption about the consistency of the characteristics of water as a working fluid can be improved by carefully analyzing the potential of the phase change (evaporation) in the well, which would modify the offered models. Other working fluids, such as supercritical CO<sub>2</sub>, can improve heat transmission between the fluid and the rocks. The analysis technique utilized in our study in conjunction with the simplified model provided in our thesis should prove to be a valuable methodological tool for determining the feasibility of converting a selected hydrocarbon well to geothermal using co-axial borehole technology.



## REFERENCES

- [1] International Energy Agency, *Renewables Information: Overview*, 2017 edition.
- [2] Kotler S. Abandoned Oil and gas Wells Are Leaking. <http://www.zcommunications.org/abandoned-oil-and-gas-wells> are-leaking-by-steven-kotler; 2011.
- [3] Cheng WL, Li TT, Nian YL, Wang CL. Studies on geothermal power generation using abandoned oil wells. *Energy* 2013; 59:248-254.
- [4] Cheng WL, Li TT, Nian YL, Xie K. Evaluation of Working Fluids for Geothermal Power Generation from Abandoned Oil Wells. *Applied Energy* 2014; 118: 238-245.
- [5] Kujawa T, Nowak W, Stachel AA. Utilization of existing deep geological wells for acquisitions of geothermal energy. *Energy* 2006; 31: 650-664.
- [6] Davis AP, Michaelides EE. Geothermal power production from abandoned oil wells. *Energy* 2009; 34: 866-872
- [7] Jeremy Boak, Alan J Cohen, Salah Faroughi, Hamed Soroush and Maria Richards. "Geothermal Energy – A Sustainable Alternative to Well Abandonment", CSEG RECORDER 2021.
- [8] Signhild Gehlin. "Geothermal energy use in the Nordic countries", *Rehva Journal* 2019.
- [9] Wang, K., Yuan, B., Ji, G., Wu, X., A comprehensive review of geothermal energy extraction and utilization in oilfields, *Journal of Petroleum Science and Engineering* (2018).
- [10] Chiasson, A.D., 2016. *Geothermal heat pump and heat engine systems: Theory and practice*, 1st ed, Wiley. John Wiley & Sons Ltd.
- [11] Liu, X., Falcone, G., Alimonti, C., 2018. A systematic study of harnessing low-temperature geothermal energy from oil and gas reservoirs. *Energy* 142, 346–355. <https://doi.org/10.1016/j.energy.2017.10.058>
- [12] Shejiao Wang, Jiahong Yan, Feng Li, Junwen Hu and Kewen Li. "Exploitation and Utilization of Oilfield Geothermal Resources in China", *Energies* 2016.
- [13] Magoon, L.B.; Dow, W.G. The petroleum system. In *The Petroleum System—From Source to Trap*; AAPG: Tulsa, OK, USA, 1994; pp. 3–24.
- [14] Bertello, F.; Fantoni, R.; Franciosi, R.; Gatti, V.; Ghielmi, M.; Pugliese, A. From thrust-and-fold belt to foreland: Hydrocarbon occurrences in Italy. In *Petroleum Geology: From Mature Basins to New Frontiers*, Proceedings of the 7th Petroleum Geology Conference; Geological Society of London: London, UK, 2010; pp. 113–126, doi:10.1144/0070113.
- [15] Zappaterra, E. Source-rock distribution model of the Periadriatic Region. *AAPG Bull.* 1994, 78, 333–354.
- [16] Ziegler, P.A.; Roure, F. Petroleum systems of Alpine-Mediterranean fold belts and basins. In *The Mediterranean Basins: Tertiary Extension within the Alpine Orogen*; Durand, B., Jolivet, L., Horvnt, E., Sèranne, M., Eds.; Geological Society: London, UK, 1999; pp. 517–540.
- [17] Jenkyns, H.C. Geochemistry of oceanic anoxic events. *Geochem. Geophys. Geosyst.* 2010, 11, Q03004, doi:10.1029/2009GC002788.
- [18] Elena Soldo, Claudio Alimonti and Davide Scrocca. "Geothermal Repurposing of Depleted Oil and Gas Wells in Italy", *Proceedings* 2020, 58, 9; doi:10.3390/WEF-06907.
- [19] Boban, L.; Miše, D.; Herceg, S.; Soldo, V. Application and Design Aspects of Ground Heat Exchangers. *Energies* 2021, 14, 2134. <https://doi.org/10.3390/en14082134>
- [20] Ioan Sarbu. "Using Ground-Source Heat Pump Systems for Heating/Cooling of Buildings", *Advances in Geothermal Energy* (pp.1-36) Chapter: 1, 2015.

- [21] Michal Kaczmarczyk, "Sustainable Utilization of Low Enthalpy Geothermal Resources to Electricity Generation through a Cascade System" al .2020.
- [22] Gudmundsson, J.; Freeston, D.; Lienau, P. The linal diagram. *GRC Trans.* 1985, 9, 15–17.
- [23] Operacz, A.; Chowaniec, J. Prospective of geothermal water use in the Podhale Basin according to geothermal step distribution. *Geol. Geophys. Environ.* 2018, 44, 379–389.
- [24] Gong YL, Luo C, MA WB, WU ZJ. Thermodynamic analysis of geothermal power generation combined fash system with binary cycle, *Proceedings World Geothermal Congress, 2010, Bali, Indonesia; 25–29 April; 2010.*
- [25] Valdimarsson P. Geothermal power plant cycles and main components, United Nation University, Geothermal training programme organized by UNP-GTP and LaGeo, in Santa Tecla, El Salvador, January 16–22. p. 1–24.
- [26] M. El Haj Assad, E. Bani-Hani and M. Khalil. "Performance of geothermal power plants (single, dual, and binary) to compensate for LHC-CERN power consumption: comparative study", *Geotherm Energy* (2017) 5:17.
- [27] DiPippo R. Geothermal energy as a source of electricity: a worldwide survey of the design and operation of geothermal power plants, U.S. Dept. of Energy, DOE/RA/28320-1. Washington, DC: Gov. Printing Ofce; 1980.
- [28] Alimonti et al. "Coupling of energy conversion systems and wellbore heat exchanger in a depleted oil well" *Geotherm Energy* (2016) 4:11.
- [29] Eugenio Trumpy, Adele Manzella. "Geothopica and the interactive analysis and visualization of the updated Italian National Geothermal Database". *International Journal of Applied Earth Observation and Geoinformation.* Volume 54, Feb 2017, pages 28-37.
- [30] Jerzy Wołoszyn. "A review of selected analytical and numerical models of borehole heat exchanger", September 2013.
- [31] Hart D.P., Couvillion R.: *Earth Coupled Heat Transfer.* Publication of the National Water Well Association, 1986
- [32] Carslaw H.S., Jaeger J.C.: *Conduction of heat in solids.* 2nd ed. London: Oxford University Press; 1959.
- [33] Eskilson P.: *Thermal analysis of heat extraction boreholes.*, PhD thesis. Sweden: University of Lund; 1987.
- [34] Yang H., Cui P., Fang Z.: *Vertical-borehole ground-coupled heat pumps: A review of models and systems.*, *Applied Energy* 2010; 87; 16–27
- [35] Guichen Li, Jianzhi Yanga, Xiaowei Zhu, Zhihe Shena. "Numerical study on the heat transfer performance of coaxial shallow borehole heat exchanger", *Energy and Built Environment* 2021.
- [36] D. Sui. "Review and investigations on geothermal energy extraction from abandoned petroleum wells". *Journal of Petroleum Exploration and Production Technology* (2019) 9:1135–1147.
- [37] Indra Noer Hamdhan and Barry G. Clarke. "Determination of Thermal Conductivity of Coarse and Fine Sand Soils", *Proceedings World Geothermal Congress 2010.*
- [38] Yaobin Zhang. "Numerical Simulation of Shallow Geothermal Field in Operating of a Ground Source Heat Pump System—A Case Study in Nan Cha Village, Ping Gu District, Beijing", *Water* 2020, 12, 2938; doi:10.3390/w12102938.
- [39] Georgios Florides, Soteris Kalogirou. "Ground heat exchangers—A review of systems, models and applications", *Renewable Energy* 32 (2007) 2461–2478.
- [40] Elif Balkan, Kamil Erkan and Müjgan Şalk. "Thermal conductivity of major rock types in western and central Anatolia regions, Turkey", *J. Geophys. Eng.* 14 (2017) 909–919 (11pp).

- [41] Boning Tang, Chuanqing Zhu, Ming Xu, Tiange Chen and Shengbiao Hu. "Thermal conductivity of sedimentary rocks in the Sichuan basin, Southwest China", *Energy Exploration & Exploitation* 2019, Vol. 37(2) 691–720.
- [42] Xiong J, et al., Investigation on thermal property parameters characteristics of rocks and its influence factors, *Natural Gas Industry B* (2020), <https://doi.org/10.1016/j.ngib.2020.04.001>
- [43] Douglas Waples. "A Review and Evaluation of Specific Heat Capacities of Rocks, Minerals, and Subsurface Fluids. Part 1: Minerals and Nonporous Rocks" *Natural Resources research*, June 2004.
- [44] Ladislaus Rybach. "Determination of specific heat capacity on rock fragments", *Geothermics* · February 2001.
- [45] Keith Hirsche and Joan Embleton. "Geothermal Energy – A Sustainable Alternative to Well Abandonment", *CSEG RECORDER*, January 2021.